3. Spinels in most of the cumulates are significantly more Cr-rich and/or Mg-poor than those in the basalts which also display much more restricted compositional variation (Fig. 5.3).

Because the PBOC low-Ti basalts are significantly depleted in Ni and Cr relative to other Ti-poor basaltic rocks (see above), it is possible that they experienced at least some olivine ± spinel fractionation. Most of the PBOC olivine-rich cumulates have lower *M* (Mg*) values (<86, e.g. Table 5.1) than might be expected of derivatives from the more Mg-rich low-Ti basalts (with *M* liquid > 65 the *M* values of any PBOC-type cumulates [(which are devoid of primary Fe-Ti oxides) would be > 86 [*cf.* Roeder and Emslie, 1970; compare *M*, Mg*, *mg* for PBOC silicates (Fig. D-2) and oxides (Fig. D-1)]. Furthermore, if olivine + spinel ± orthopyroxene fractionation had been operative, with decreasing *M* more evolved derivatives would be expected to display well-defined trends of progressively increasing Al, Ca, and incompatible elements (e.g. Ti, P, Zr, Y), and rapidly decreasing Ni. Although the general trends of decreasing Al and Ca with decreasing *M* in the PBOC low-Ti basaltic rocks (Fig. 5.15) may partly reflect albitization of plagioclase (see above), as a group these rocks display the following characteristics which are also at variance with their derivation from a common parent or similar parents by olivine + spinel ± orthopyroxene fractionation controls: (i) irregular and restricted variations in relatively immobile elements such as Ti, P, Zr, Y, Cr and Ni with decreasing *M* (Table 5.6a); (ii) only limited depletion in Ni (150 µg/g-80 µg/g) for a substantial decrease in *M* (71-58; *cf.* Sato, 1977) and (iii) irregular Cr:Y relations (Fig. 6.1h, *cf.* Pearce, 1980). The irregular and restricted variation in Cr/(Cr + Ni) ratios (0.6-0.8, *cf.* Flower *et al.*, 1977) coupled with the complete lack of non-quench Ca-rich pyroxene phenocrysts in the PBOC low-Ti basaltic rocks (Section 5.7.2) also suggest that any fractionation of clinopyroxene (most unlikely) was in fact negligible.

Similarly, magma mixing (*cf.* O'Hara, 1977; O'Hara and Matthews, 1981) is probably not a viable model to explain the observed chemical variations in the PBOC low-Ti basaltic rocks because it would also tend to produce well-defined trends of increasing incompatible element abundances with decreasing *M*. Rather, the chemistry of these basaltic rocks is perhaps best explained if some (possibly most) of the liquids they now represent were in fact a number of discrete primary or only slightly fractionated partial melts from unusual, incompatible element-depleted, but not necessarily highly refractory, upper mantle source rock(s).

Largely on the basis of the refractory compositions of oceanic and ophiolitic tectonized (depleted) harzburgites ($M \geq 90$) and the widely-held view that the upper mantle has a bulk M value of 88-90 (e.g. Frey *et al.*, 1978; Jaques and Green, 1980; Maaløe and Steele, 1980; see references in O'Nions *et al.*, 1981), with some exceptions (see below) current hypotheses on the genesis of MORB and ophiolitic basalts generally favour a model whereby these are ultimately derived from Mg-rich basaltic ($M \sim 70$) or picritic ($M > 70$) liquids largely *via* the fractionation of olivine + spinel ± clinopyroxene ± plagioclase (e.g. O'Hara, 1968; Langmuir *et al.*, 1977; Bender *et al.*, 1978; Byerly and Wright, 1978; Bryan, 1979; Elthon, 1979; Duncan and Green, 1980a,b; Elthon and Scarfe, 1980; Stolper, 1980; Stolper *et al.*, 1981; Beets *et al.*, 1982). From a similar standpoint, many ophiolitic Ti-poor basaltic rocks are also considered to have evolved from relatively Mg-rich melts (for which extrusive analogues might exist in some ophiolites, e.g. Betts Cove, Coish and Church, 1979; and Troodes see points 24, Fig. 5.13) *via* some fractionation of Mg-rich phases such as olivine ± orthopyroxene, although there is some disagreement on other aspects of their genesis. Numerous authors (e.g. Sun and Nesbitt, 1978; Cameron *et al.*, 1979; Cameron, 1980; Meijer, 1980; Crawford *et al.*, 1981; Tatsumi, 1981, 1982; Hickey and Frey, 1982) maintain that Ti-poor basaltic rocks, particularly boninites, are generated by hydrous partial melting of a depleted peridotite source. On the other hand, Duncan and Green (1980a,b) propose that at least some rocks of this type could be generated by small degrees (5-10%) of anhydrous melting of refractory peridotite diopirs at relatively shallow depths ($\leq$ 25 km). This proposal is supported by the experimental data of Jaques and Green (1980) whereby Mg-rich tholeiite and Mg-rich quartz tholeiite liquids were produced by low degrees (< 20%) of anhydrous partial melting of a depleted (Tinaquillo) spinel 'lherzolite' at relatively low pressures (2-15 kb).

Because the melts now represented by the PBOC low-Ti basaltic rocks (and, for that matter, almost all other envisaged PBOC melts) appear to have been highly depleted in incompatible elements and essentially anhydrous, in some respects the second-stage melt model advocated by Duncan and Green (1980a, b) and Jaques and Green (1980) might be genetically viable. However, anhydrous partial melts of the Tinaquillo 'lherzolite' (Table 5 in Jaques and Green, 1980) whose TiO_2, Al_2O_3 and CaO contents are similar to the more Mg-rich PBOC low-Ti basalts (e.g. melts 1-3, Figs 5.13, 5.14) are significantly enriched in Mg (13-15% MgO) relative to the latter, and/or have significantly higher M values (74-78).

If, on the basis of earlier evidence, it is accepted that progressive olivine + spinel ± orthopyroxene fractionation and/or magma mixing are not responsible for the chemical variations displayed by the PBOC low-Ti basaltic rocks as a whole, it becomes necessary to consider the possibility that each individual PBOC low-Ti basaltic cooling unit might represent a largely discrete pulse of relatively Mg-, Ni-, Cr-, and perhaps Si-rich, Ti-poor basaltic melt (*cf.* Duncan and Green, 1980a,b) which was derived from an extremely depleted, perhaps highly refractory mantle source(s). These subsequently could have evolved separately to melts with variable lower *M* values largely *via* the fractionation of phases relatively rich in Mg and perhaps Si (i.e. olivine ± orthopyroxene). Alternatively, the liquids represented by the more Mg-rich PBOC low-Ti basaltic rocks (e.g. $M > 60$) might have been primary melts in equilibrium with a slightly more Fe-rich mantle source (M = ? 82-88)* than commonly envisaged ($M \sim 90$), and which had experienced several earlier episodes of partial melting.

Concerning the former alternative, it is conceivable that some of the PBOC orthopyroxene-bearing cumulates, specifically the cumulate harzburgites (Section 5.2), the olivine orthopyroxenites (Section 5.3.1), and perhaps other (rare) Mg-rich ($M > 88$, see below) variants (Section 5.3) might be precipitates from melts parental (with $M > 71$) to one or other of the PBOC low-Ti basaltic units. In the PBOC cumulates as a whole, however, orthopyroxenes display a more extensive range in *mg* values (*mg* = 91-62, with *mg* more-or-less continuous in the range 91-72, e.g. Fig. 5.5) than would be expected if this mode of origin is applicable to any significantly orthopyroxene-bearing PBOC cumulates with *M* values less than 88. That is, orthopyroxenes in the PBOC cumulates presumably crystallized from melts whose *M* values generally ranged from 76 to 45, and on occasion were as low as (?) 30 (see opx-ol-liquid Fe:Mg relations, p. 221; *cf.* Nielsen and Drake, 1979). However, the complete absence of (phenocrystal) modal orthopyroxene from the low-Ti basaltic units (M = 71-58) suggests that orthopyroxene obviously was not a fractionating phase for these compositions. Of course, this does not preclude the possibility that some of the PBOC dunitic cumulates with *M* values less than 88 (M = 88-85, e.g. 473) crystallized from one or other of the 'low-Ti basaltic melts' whose *M* values are now less than $\sim$ 68. The available data place few further constraints on this model. Because olivine phenocrysts (pseudomorphed)

---

* Assuming $D_{Fe\text{-}Mg}^{ol\text{-}liq} \sim 0.30\text{-}0.33$; for discussions see Wilkinson (1982) pp. 10-11 and Basaltic Volcanism Study Project (1981), pp. 418-419.

are rare in even the most Mg-rich PBOC low-Ti basaltic rocks, and because the relatively Fe-rich variants are completely devoid of evidence for the former presence of olivine (Section 5.7.2), any olivine, or for that matter orthopyroxene (if indeed these were liquidus phases), must have been very efficiently removed from primitive PBOC 'low-Ti basaltic melts' prior to final crystallization.

In the light of currently popular concepts on the composition of basalt source areas in the upper mantle (M > 88, see above) and on the compositions of primary magmas (M > 70, see above) derived from these source areas, a primary origin for the melts now represented by the PBOC low-Ti basaltic (M = 71-58) rocks might seem unlikely. Nevertheless, some experimental data (e.g. Kushiro and Thompson, 1972; Fujii *et al.*, 1978) and empirical observations suggest that many basalts whose M values are significantly less than 70 (e.g. MORB T-87, $M \sim 66$, Kushiro and Thompson, 1972) might represent primary melts from relatively Fe-rich mantle source regions (for reviews see Wilkinson, 1980,1982; Fujii and Bougault, 1983). Although the available data are not entirely definitive, some aspects of the chemistry of the PBOC low-Ti basaltic rocks suggest that at least a majority of these could also be primary. Perhaps the least ambiguous characteristics are the 'normal' basaltic major element chemistries and moderate M values (*cf.* MORB) despite extreme depletion in Ti, P, and Zr, significant depletion in Y, Nb and REE (5-10x chondrites, assuming Y ≡ Ho, e.g. Frey *et al.*, 1968) and, bearing in mind possible alteration effects, significant depletion in K and Ba. By comparison, similarly-depleted low-Ti 'basalts' (SiO_2 < 54%) in ophiolites typically have significantly higher M values (M = 70-80) and MgO contents (> 10%), lower Al/Mg ratios (e.g. Fig. 5.13A,C) and, for the most part, lower Al_2O_3 contents (generally 10-14% Al_2O_3, *cf.* Table 5.6a). Using the comparable incompatible element abundances as a guide to source rock chemistry, the Mg, Mg:Fe, and Al characteristics of the ophiolite examples presumably reflect partial melting of sources relatively rich in Mg and poor in Al (and Fe?), compared with PBOC source rocks. If fractionation of relatively Mg-rich phases was the dominant factor controlling chemical variations in low-Ti basaltic rocks, then the world-wide rarity (?virtual non-existence) of 'evolved' variants [$M \ll 70$; e.g. analyses 12-14, Table 5.6a for which $58 \leqslant M \leqslant 60$ and Zr = 8-10µg/g, and perhaps several moderately-highly altered doleritic dykes in the Aspropotamos sequence, Pindos, for which M = 72-55 and Zr = 6-25µg/g (Capedri *et al.*, 1980)] whose incompatible element abundances are predictably low (these are likely to remain "low" for moderate levels of fractionation, e.g. < 50%) is, to say the least, surprising!

It is probably reasonable to assume that the source area(s) for the PBOC low-Ti basaltic melts was/were depleted in incompatible elements following one or more partial melting episodes (*cf.* Sun and Nesbitt, 1978; Duncan and Green, 1980a,b). Consequently, from the above discussion, and because *M* values of mantle residua increase relatively rapidly with increasing degrees of partial melting, it is possible that the undepleted source rocks of the PBOC melts had *M* values as low as ∿ 80-82. Furthermore, if these hypothetical source regions were originally relatively clinopyroxene-rich, residual clinopyroxene involved in "low-Ti melt generation" might account for the unusually low Ti/V* (Fig. 6.1j) and Zr/Y (Fig. 5.16, *cf.* Pearce and Norry, 1979) ratios, and the relatively high Sc abundances (*cf.* Glassley and Piper, 1978) in the PBOC low-Ti basaltic rocks. The entry of garnet into these melts might result in similar characteristics (at least for Zr/Y and Sc). However, garnet participation would also be expected to produce significantly greater HREE/LREE ratios than those displayed by PBOC low-Ti basaltic rocks (which are probably ∿ 1, assuming Y ≡ Ho and that Ce is relatively immobile or enriched during alteration, see Section 3.5.1; Lambert and Holland, 1974), and, conceivably, lower Ti/Zr ratios ($D_{Ti,\,Zr}^{garnet-liq}$ ∿ 0.3, $D_{Ti}^{cpx-liq}$ ∿ 0.3, $D_{Zr}^{cpx-liq}$ ∿ 0.1, Pearce and Norry, 1979). In any case, the moderate to high (for basalts) SiO_2 contents of these rocks (50-50.5% SiO_2) suggest that they were most probably generated at lower pressures (≲ 10 kb?, *cf.* De Paolo, 1979; Duncan and Green, 1980a; Jaques and Green, 1980) than those at which garnet is stable under upper mantle conditions (? > 12-15 kb). Furthermore, the relatively high Na and Sr abundances relative to incompatible and LIL elements in most of these rocks (see Table 5.6a) might suggest that plagioclase was present in their source region(s) (? plagioclase lherzolite-spinel lherzolite transition zone), that is, they were generated at pressures <∿ 10 kb (e.g. Green and Hibberson, 1970; Ringwood, 1975; *cf.* Menzies and Allen, 1974; Presnall *et al.*, 1979; Sen, 1982; Wilkinson, 1982; Fujii and Bougault, 1983). However, because the original Na and Sr abundances may have been modified to varying degrees following alteration (e.g. albitization of plagioclase, see earlier comments; note broad range of Sr:Ti and Sr:Zr ratios, Fig. 6.1b, *cf.*

---

* $D_{Ti}^{cpx-liq}$ ∿ 0.3-?0.5 (Pearce and Norry, 1979; Shervais, 1982), $D_{V}^{cpx-liq}$ ∿ 5 for low fO_2 (Shervais, 1982). However, the Ti/V ratios of melts might also be decreased if significant amounts of spinel were consumed during partial melting (*cf.* Ti/V ratios > 1 for spinels in PBOC tectonized harzburgites, pp. 8-9 of Table C-2). By contrast with the PBOC low-Ti basaltic rocks, the low Ti/V ratios in boninites and IAT appear to reflect relatively high fO_2 conditions during their generation (Shervais, 1982).

Smith and Smith, 1976), any conclusions utilizing these elements of necessity must be tentative.

Recent experimental data indicate that MORB melts with M values slightly less than 70 may be in equilibrium with relatively low-pressure upper mantle assemblages (i.e. ol + opx + cpx ± spinel ± plagioclase; see Fujii and Bougault, 1983 for a review). It is therefore conceivable that the more Mg-rich PBOC low-Ti basaltic compositions (? $M > 65$) might reflect primary compositions, following the extraction from the undepleted source rocks of an incompatible element-enriched melt(s) (*vide* the multi-stage melting concept of Duncan and Green, 1980a,b). However, on the evidence presently available, the genesis of the more Fe-rich variants (M = 65-58; analyses 10-14, Table 5.6a) is tentatively assigned to that model which currently enjoys the widest petrological consensus, namely olivine ± spinel ± orthopyroxene fractionation from more Mg-rich parental melts (not necessarily represented in the PBOC) with uncharacteristically low abundances of the more common incompatible elements.

5.8 GENERAL SUMMARY AND CONCLUDING REMARKS

5.8.1 Summary and Comments

The PBOC is a highly disrupted and relatively poorly preserved ophiolitic melange essentially confined to major fault systems in the Pigna Barney-Curricabark area, southern NEO. It borders and is in tectonic contact with parts of the Tamworth Belt, and the Woolomin and Nambucca associations. Salient petrological characteristics of the PBOC, some of which are peculiar to this complex, include the following:

Critical Lithological Components

(i) An unusually *en*/OPX-rich tectonized harzburgite member, perhaps in this respect comparable only to tectonized harzburgites in the Papuan Ultramafic Belt (PUB, *cf.* England and Davies, 1973; Jaques and Chappell, 1980).

(ii) Cumulate harzburgites and rare cumulate olivine orthopyroxenites, all of which contain remarkably Mg-rich olivine and orthopyroxene [mg = 92-90; *cf.* cumulus ol ($mg \leq 93$) and opx ($mg \leq 94$) in the Marum Ophiolite, PUB (Jaques, 1981) and in the Adamsfield Ultramafic Complex, Tasmania (Varne and Brown, 1978)]. These PBOC harzburgites contain spinels which are unusually Al-rich for cumulates (Cr = 40-25) whereas, in

contrast, spinels in the olivine orthopyroxenites are unusually Cr-rich ($Cr \sim 84$) for their relatively low M values ($M \sim 34$).

(iii) A group of plagioclase-bearing 'harzburgites' and 'dunites' whose olivines display a limited and somewhat atypical (for these modal compositions) Fe-rich range in Fo (Fo_{88-84}). Comparable plagioclase-bearing peridotites appear to be relatively rare in ophiolites (e.g. Coleman, 1977; Church and Riccio, 1977).

(iv) Abundant olivine (mela-) norites whose textures and individual phase chemistries strongly suggest that they may have been produced by convective fractionation processes (Rice, 1981) rather than by simple crystal accumulation, the latter origin being widely accepted for most ophiolitic cumulates (but perhaps subject to reinterpretation in many cases, *cf.* Casey and Karson, 1981; Irvine, 1982). Furthermore, the crystallization sequence in these olivine norites and the PBOC cumulates as a whole (Cr-Al spinel → olivine → orthopyroxene → plagioclase → clinopyroxene) is itself highly unusual (Church and Riccio, 1977), as is the persistence of Cr-Al spinel in place of any Fe-Ti oxides in the more Fe-rich variants (implying relatively high Cr and low fO_2 in the parental liquid(s)].

(v) Cumulate gabbros (gabbronorites) in which primary quartz may coexist with relatively Mg-rich orthopyroxenes (e.g. En_{79-75}), suggesting that the parental liquids were significantly *hy*- and *qz*-rich.

(vi) Minor relatively quartz-rich, Ti-poor, orthopyroxene-free doleritic intrusives whose genetic relations with the other components of the PBOC are at present enigmatic.

(vii) A group of little-altered, orthopyroxene-free low-Ti basaltic extrusives and related high-level intrusives whose chemistry suggests initial derivation by relatively low pressure (? ∿ 8-10 kb) partial melting of highly depleted (with respect to the incompatible elements), but not necessarily highly refractory (in terms of M value, and Ca, Al, and perhaps Na abundances; see discussion, pp. 248-256), clinopyroxene-bearing mantle source rocks. Although these low-Ti eruptives bear the general petrological stamp of low-Ti ophiolitic basalts (*cf.* Sun and Nesbitt, 1978), they differ in various details of their petrography and chemistry from all other known examples of this type.

Generalized Petrological Characteristics

With the occasional exception of some minor quartz-bearing doleritic intrusives:

(viii) The primary chemistry of all ophiolitic members of the PBOC is characterized by exceptionally low incompatible element (e.g. Ti, P, Zr, Y, Nb) abundances and Ti/V, Zr/Y, Zr/Nb ratios, low K, Rb, Ba, Sr and REE abundances, moderately high abundances of Mg, Cr and Ni, and substantial normative *hy*/OPX (usually > 20%).

(ix) With very rare exceptions (i.e. the vesicular extrusives and the more Fe-rich gabbros), ophiolitic members of the PBOC are entirely devoid of primary Fe-Ti oxides. This indicates low fO_2 and, by implication, low aH_2O in the parental magmas.

(x) The olivine norite cumulates and low-Ti basaltic rocks have unexpectedly high (for such 'depleted' compositions) $^{87}Sr/^{86}Sr$ ratios which fall in the range 0.704-0.705 (? ≈ initial $^{87}Sr/^{86}Sr$ because $^{87}Rb/^{86}Sr$ ratios are low ∿ 0.1, Table H-2, and the age of the rocks is not great, ? ∿ 400 m.y.). Although the $^{87}Sr/^{86}Sr$ ratios of the basaltic variants may have been increased by alteration (*cf.* Spooner, 1976; Menzies and Seyfried, 1979; Verma, 1981), alteration effects in the particular olivine norite sample analysed (440) are likely to have been negligible (see p. 213). Relatively unaltered rocks with similarly high initial $^{87}Sr/^{86}Sr$ do occur in a number of ophiolites (e.g. Coleman, 1977), particularly those which allegedly display some island arc characteristics, e.g. the Troodos (Peterman *et al.*, 1971; Coleman and Peterman, 1975), Vourinos (Noiret *et al.*, 1981) and Khan-Taishir (Plyusin *et al.*, 1980) ophiolites. On the other hand, preliminary Nd isotopic data on PBOC olivine norite 440 (bulk $^{143}Nd/^{144}Nd$ = 0.512552, H.D. Hensel *pers. comm.*) are comparable to those displayed by basalts in continental settings (*cf.* Fig. 2 of Noiret *et al.*, 1981; Hawkesworth *et al.*, 1979; Allegre *et al.*, 1982). Hence, available isotopic data on the PBOC appear contradictory and, for the present, any implications for the origin and evolution of the PBOC remain ambiguous.

5.8.2 Concluding Remarks

Although chemical (and petrographic) evidence for a link between PBOC intrusives and extrusives *via* fractional crystallization controls is not compelling, first order similarities in chemistry are sufficient to

strongly suggest at least a common upper mantle source region(s) for their respective (parental) melts, and retention of communal chemical characteristics during any subsequent evolution. Certain specific characteristics of the PBOC (e.g. the striking depletion in incompatible elements, *cf.* 'primitive' MORB for example) invite comparisons with Ti-poor basaltic associations in a number of ophiolites and present-day fore-arc settings.

However, the PBOC is unusual, perhaps unique, in its total petrological character. Furthermore, several aspects of the detailed petrology of its various members (e.g. $Zr/Y < 1$) reinforce this uniqueness. Indeed, as more detailed data on ophiolites and ophiolitic assemblages accumulates, the more it becomes apparent that each and every example displays one or more intrinsically distinctive petrological traits (see, for example, Upadhyay and Neale, 1979; Cameron *et al.*, 1980). Consequently, criteria whereby individual ophiolites may be unambiguously assigned to specific tectonic settings must be considered, at least for the present, imprecise.

The essential character of the PBOC is that of a highly disrupted and incompletely preserved remnant of what might be termed a 'depleted'- or 'Ti-poor ophiolite'. That is, it is distinctive in that all its ophiolitic members display 'depleted' characteristics. Where they are present in ophiolitic assemblages elsewhere and in contemporary settings, 'Ti-poor' extrusives and intrusives are usually subordinate in volume and/or form part of a composite Ti-poor - relatively Ti-rich association (e.g. Troodos, Pindos, Betts Cove, PUB, West Philippine-Mariana region). Nevertheless, general comparisons with a number of these examples suggest that the PBOC probably evolved in a fore-arc or juvenile inter-arc rift setting. The extent to which the palaeotectonic setting of the PBOC is constrained by its present geological setting is discussed in Chapter 7.

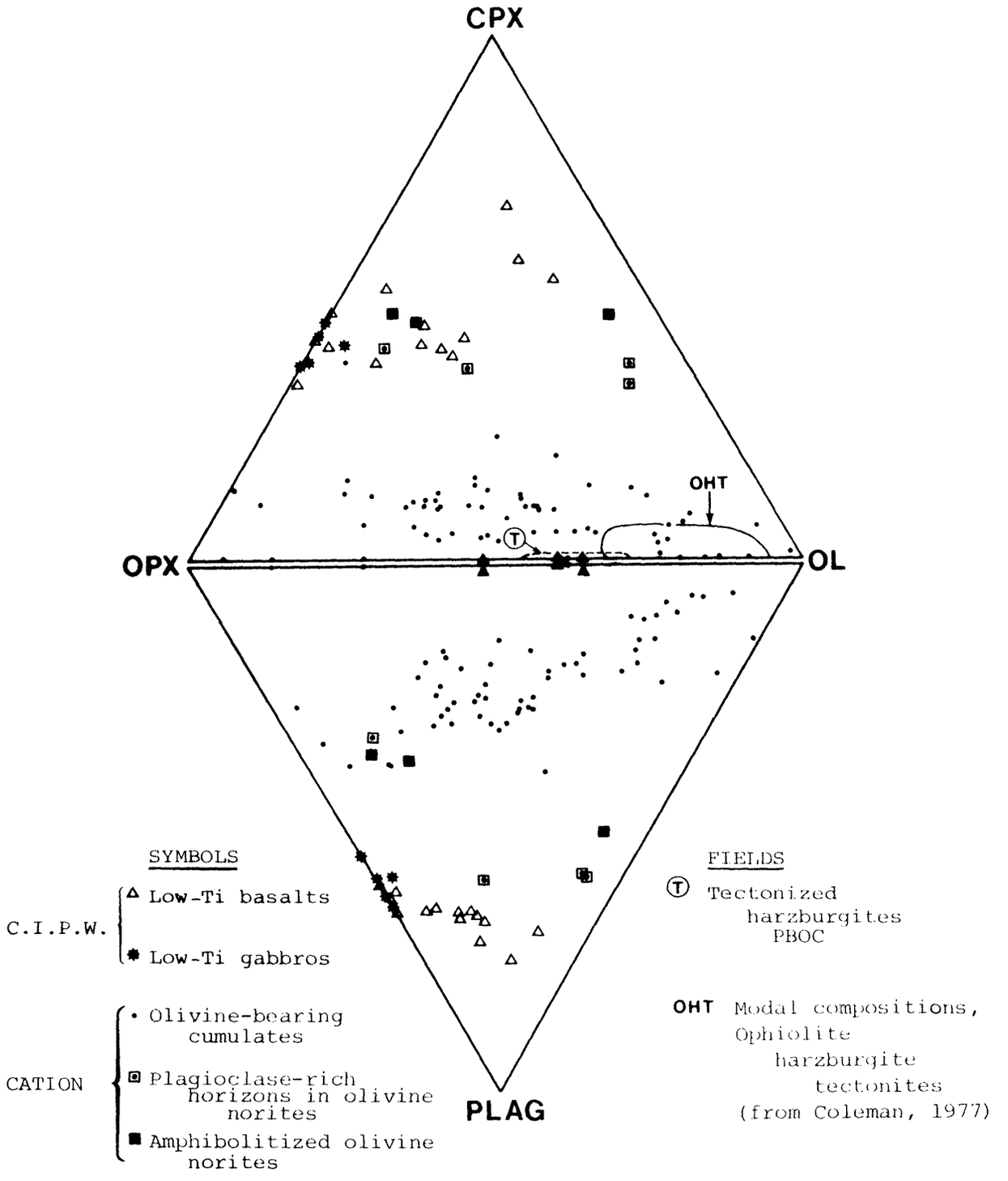

Fig. 5.2 Normative compositions of ophiolitic members of the PBOC (wt%). See Appendix A for a description of the CATION norm employed in this study.

Figure 5.3: Variations of Ti (a), V (b), Fe^{3+} (c), and *Cr* (d) as functions of *M* in Cr-Al spinels in ophiolitic members of the PBOC.

SYMBOLS:

PBOC:
- • tectonized harzburgites
- ▽ Watchimbark cumulate barzburgites
- ⊡ olivine orthopyroxenite
- ● massive chromitite
- a amphibole-bearing peridotite
- ◝ plagioclase-bearing peridotites
- t plagioclase-rich peridotites
- ▪ sedimentary serpentinite
- · olivine norites
- 1-5 low-Ti basaltic rocks

MORB: I, II, III, = early-, middle-, and late-crystallizing Cr-Al spinels in FAMOUS MORB (Fisk & Bence, 1980).

- ⬯ MORB, MAR 30°-40°N (Sigurdsson and Schilling, 1976).
- ⁂ Picrite, " " " " "
- ⬭ DSDP Leg 46 (Dick and Bryan, 1978).

all MORB: includes analyses from Frey *et al.* (1974), Ridley *et al.* (1974), Ayuso *et al.* (1976), Donaldson and Brown (1977), O'Donnell and Presnall (1980).

- P = Panton Sill (Hamlyn, 1980)
- S = stratiform intrusions, including ophiolitic examples (e.g. Irvine and Findlay, 1972)
- A = alpine ultramafics (e.g. Irvine and Findlay, 1972).
- B = boninitic rocks (Cameron *et al.* 1979)
- △ = Cr-Al spinels in Myra *Type* basaltic extrusives (see Chapter 3).
- ⓐ = PBOC plagioclase-poor amphibolites (see Chapter 6).

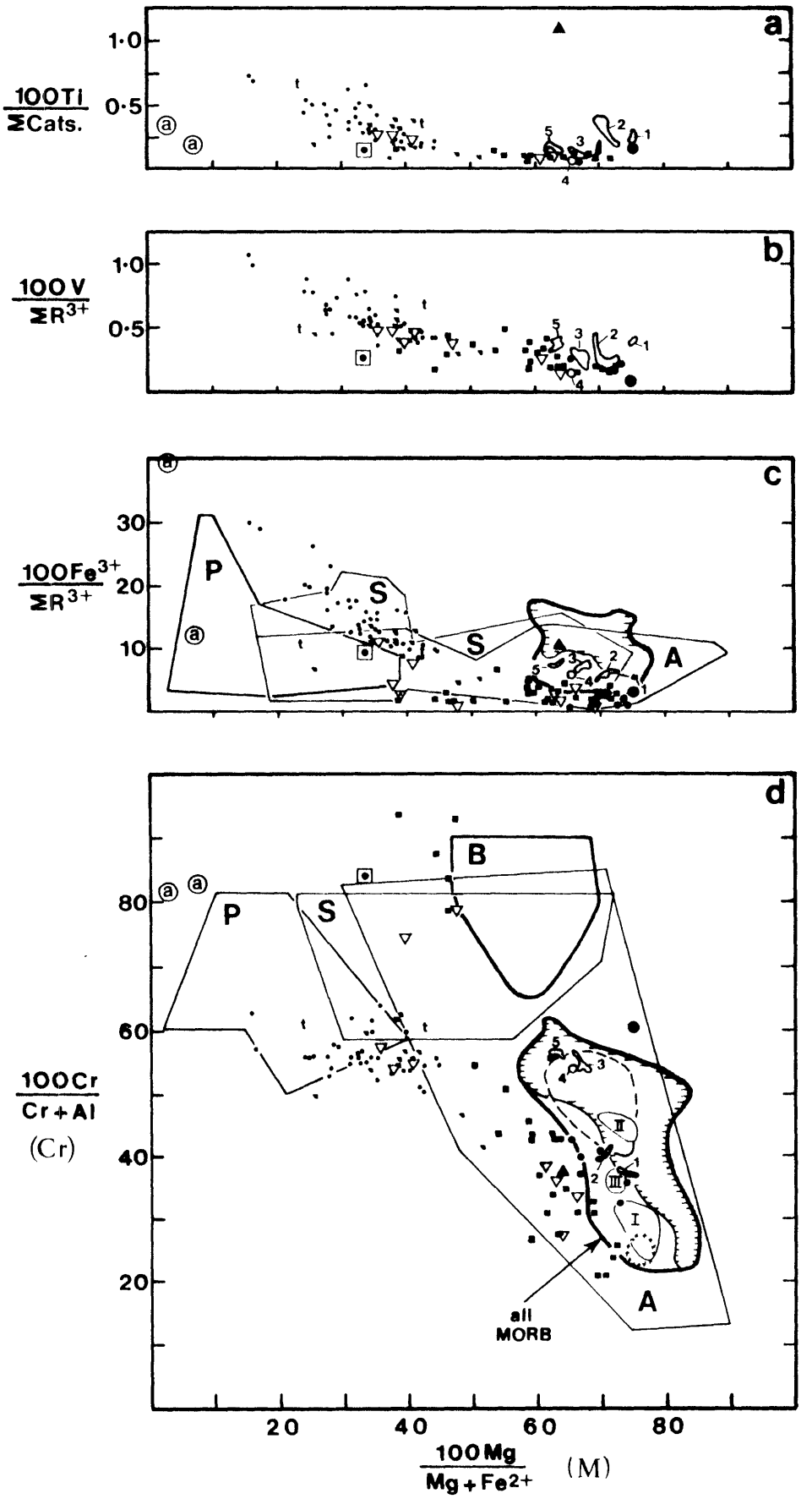
a
1·0
0·5
100Ti / ΣCats.
b
100V / ΣR3+
c
30
20
10
100Fe3+ / ΣR3+
P
S
S
A
d
B
P
S
80
60
40
20
100Cr / Cr+Al
(Cr)
all MORB
A
20
40
60
80
100Mg / Mg+Fe2+
(M)

Fig. 5.3

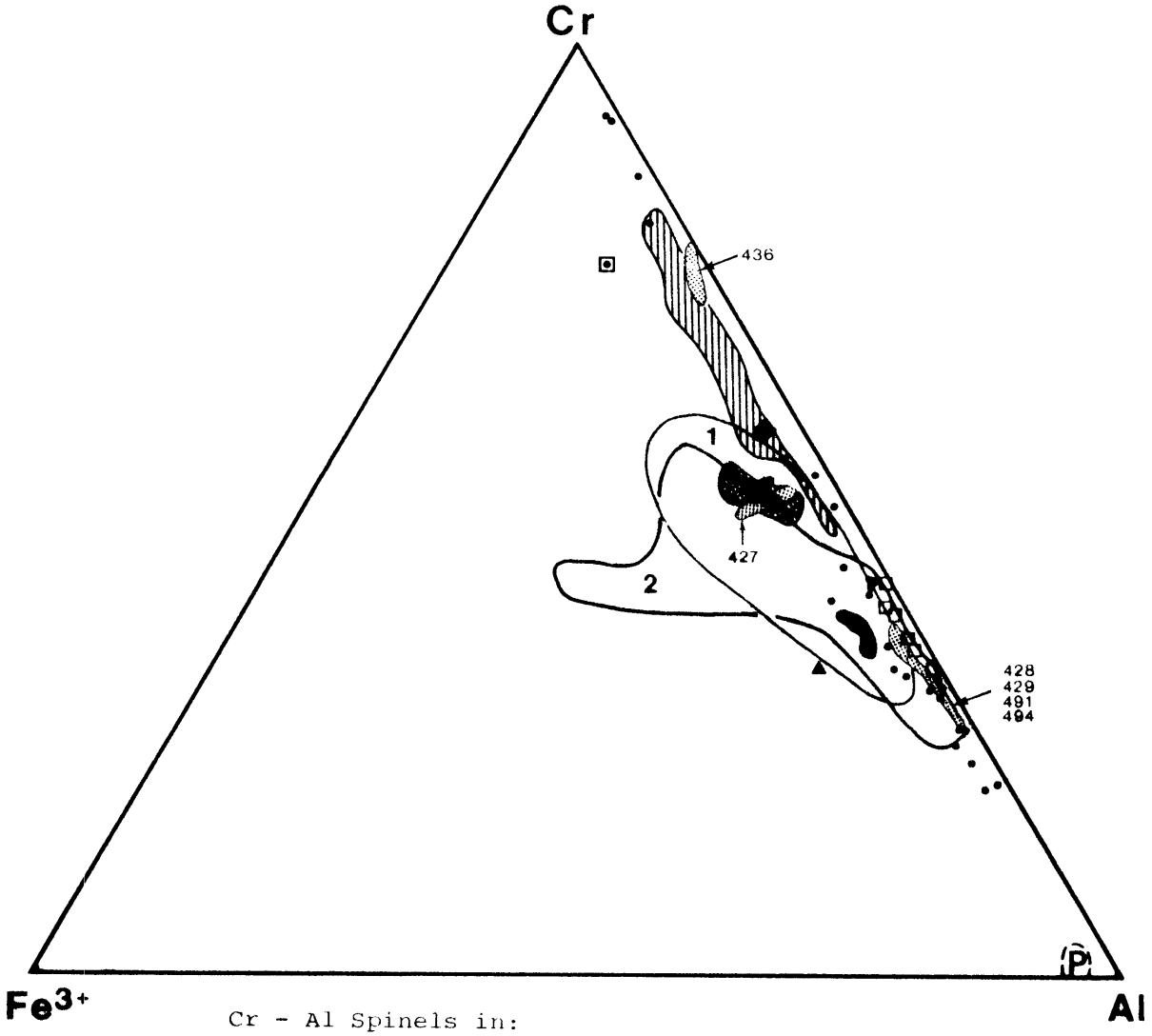

Cr - Al Spinels in:

- PBOC low-Ti basalts
- (1) MORB (field modified from Hodges and Papike, 1976)
- (2) PBOC olivine-bearing cumulate rocks
- PBOC olivine orthopyroxenite (sample 489 , ave chromite)
- PBOC tectonized harzburgites
- PBOC Watchimbark cumulate harzburgites (sample no.s listed)
- DSDP Site 334 gabbros (Hodges and Papike, 1976; Clarke and Loubat, 1977)
- (P) PBOC amphibolitized olivine-bearing intrusives (metamorphic pleonastes)
- Troodos chromitites (Greenbaum, 1977)
- PBOC massive podiform chromitite
- PBOC sedimentary serpentinites
- Myra *Type 3* basaltic extrusives (ave)

Fig. 5.4: $Cr:Al:Fe^{3+}$ relations in spinels from ophiolitic members of the PBOC and Myra *Type 3* basaltic extrusives.

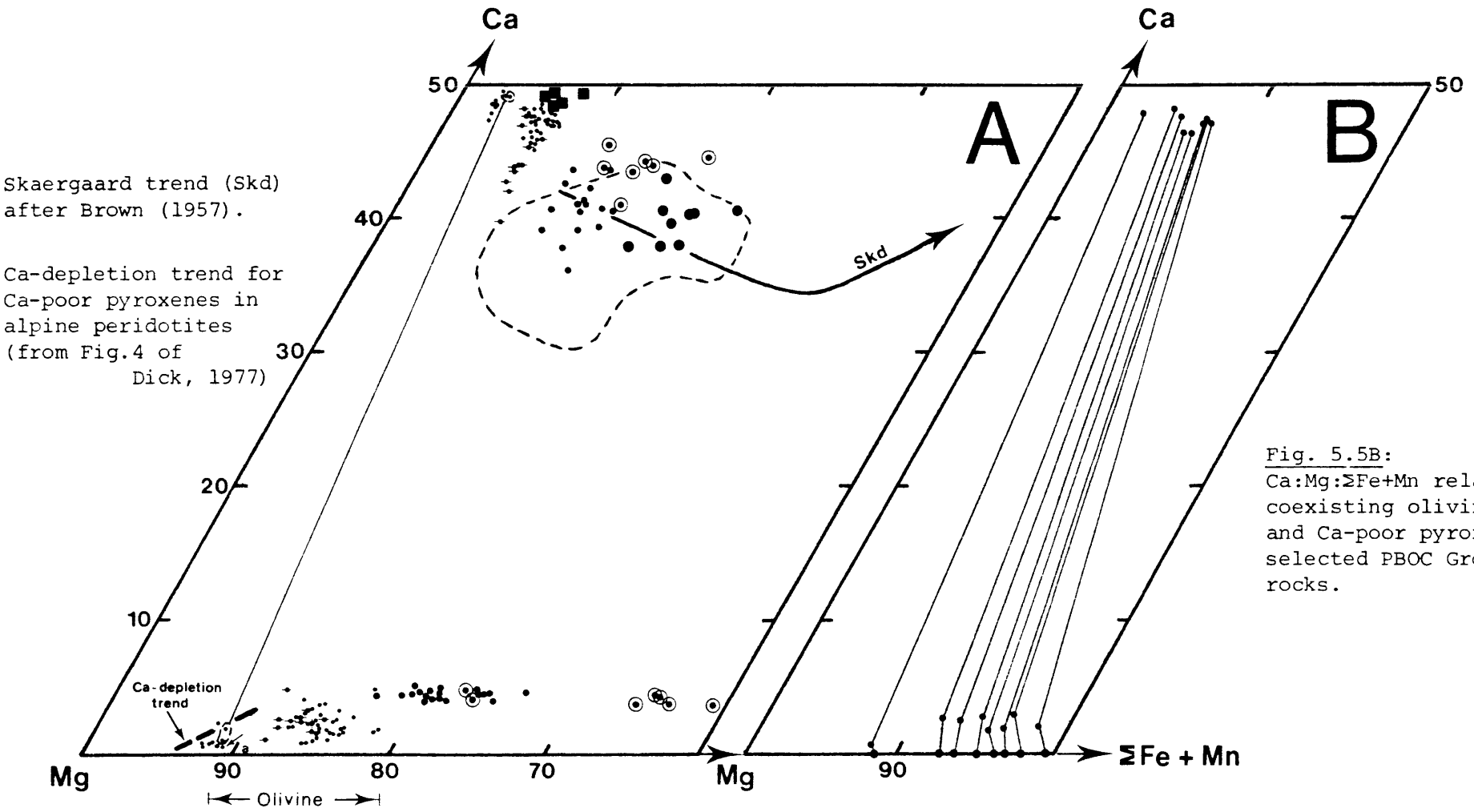

Fig. 5.5B:
Ca:Mg:ΣFe+Mn relations of coexisting olivine + Ca-rich and Ca-poor pyroxenes in selected PBOC Groups 1-4 rocks.

Fig. 5.5: Ca:Mg:ΣFe+Mn relations of pyroxenes in ophiolitic members of the PBOC and in clinopyroxene-rich cumulates from the Curricabark Fault Zone (locality 14, see Fig. B-1 and Appendix F).

A: ·= tectonized harzburgites and olivine-bearing cumulates, coexisting pyroxenes in Watchimbark cumulate harzburgites joined by tie-line, olivine orthopyroxenite arrowed, a = amphibole-bearing harzburgite, ⋆ ⋆ = plagioclase-bearing peridotites, • = low-Ti gabbros (pyroxenes from most Fe-rich sample 028 are circled), ● = low-Ti dolerites. Large dashed field = prismatic Ca-rich pyroxenes from low-Ti basalts and microdolerites. ■ = olivine clinopyroxenite and olivine gabbro.

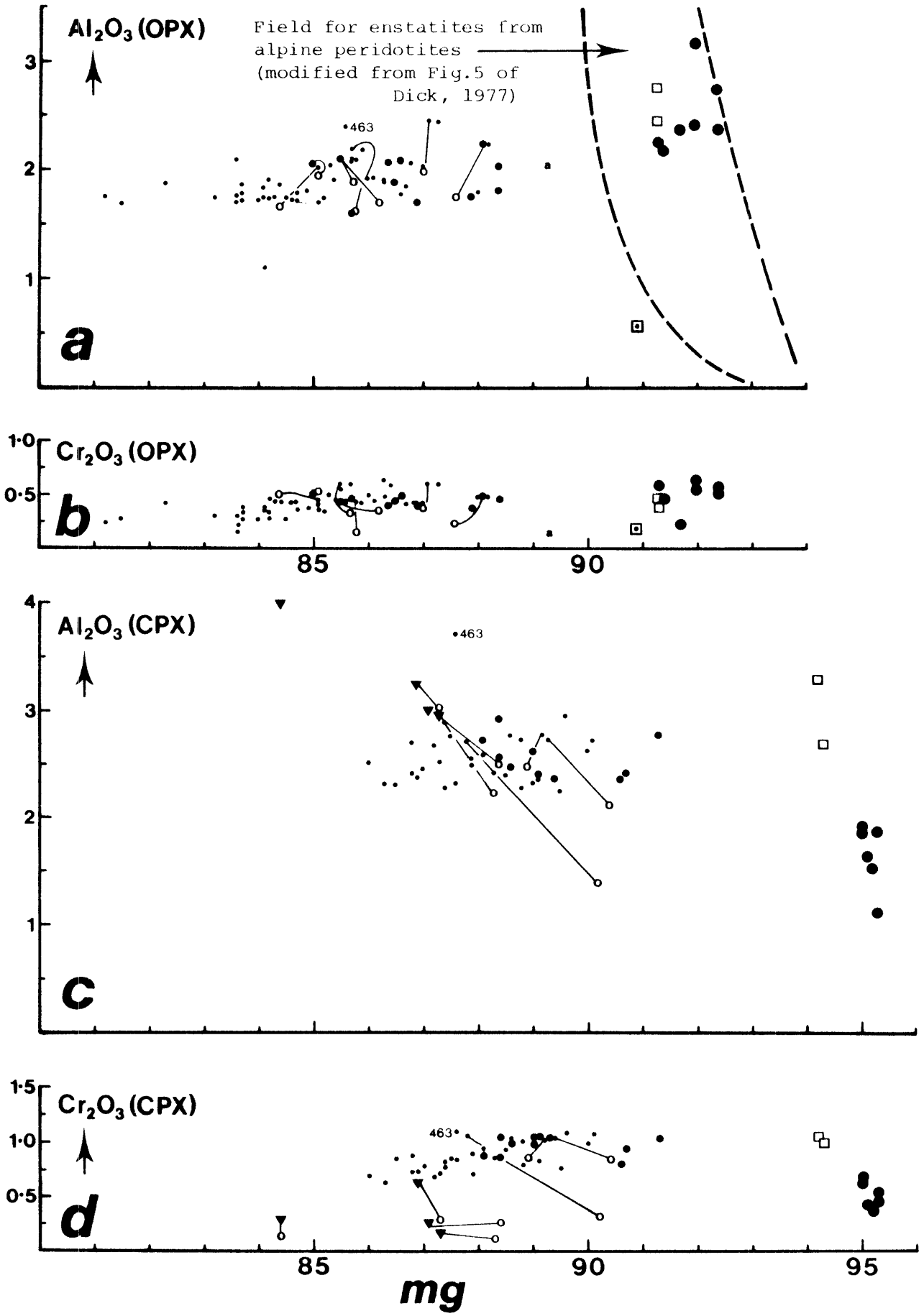

Fig.5.6: Al_2O_3 and Cr_2O_3 variations as a function of *mg* for Ca-rich and Ca-poor pyroxenes in PBOC tectonized harzburgites and olivine-bearing cumulates. PBOC: tectonized harzburgites (●), cumulate harzburgites (□), olivine orthopyroxenite (⊡), plagioclase-bearing peridotites (•), olivine norites (•); rim compositions (o), tie lines join respective cores and rims. *mg* = 100Mg/(Mg+ΣFe+Mn).
▼ = Ca-rich pyroxines from olivine clinopyroxenites and an olivine gabbro (locality 14).

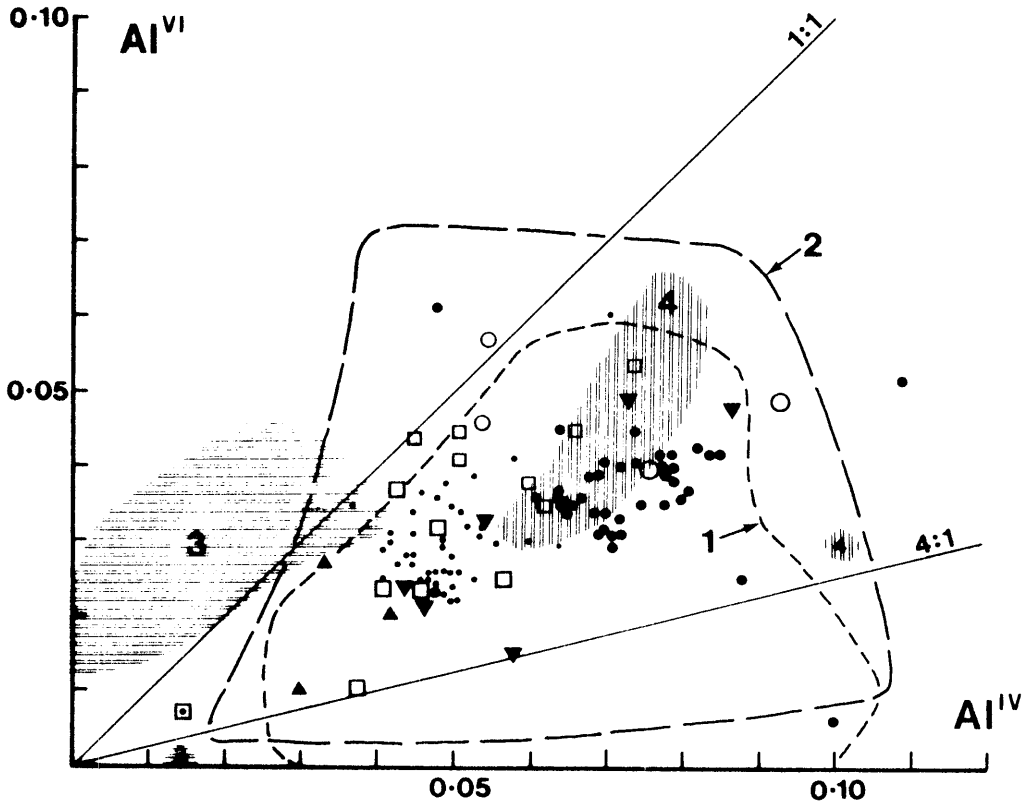

Fig. 5.7: $Al^{IV}:Al^{VI}$ relations in pyroxenes from mafic and ultramafic rocks in the PBOC. Fields 1 and 2 for orthopyroxenes and clinopyroxenes respectively from the following tectonized harzburgites: Burro Mountain (Loney *et.al.*,1971), Vulcan Peak (Himmelberg and Loney, 1973), Red Mountain, N.Z. (Sinton,1977), Canyon Mountain (Himmelberg and Loney, 1980) and the Sangun-Yamaguchi Zone, Japan (Arai, 1980). Fields 3 and 4 for orthopyroxenes in highly depleted (3) and fertile (4) Al-Cr spinel harzburgite mantle xenoliths from southern African kimberlites and alkaline basalts (Hervig *et. al.*, 1980).

PBOC	OPX	CPX	
	□	□	tectonized harzburgites
	○	○	cumulate harzburgites
	·	•	olivine norites and miscellaneous cumulate rocks
	▲	▼	cumulate gabbros
	⊡		olivine orthopyroxenite

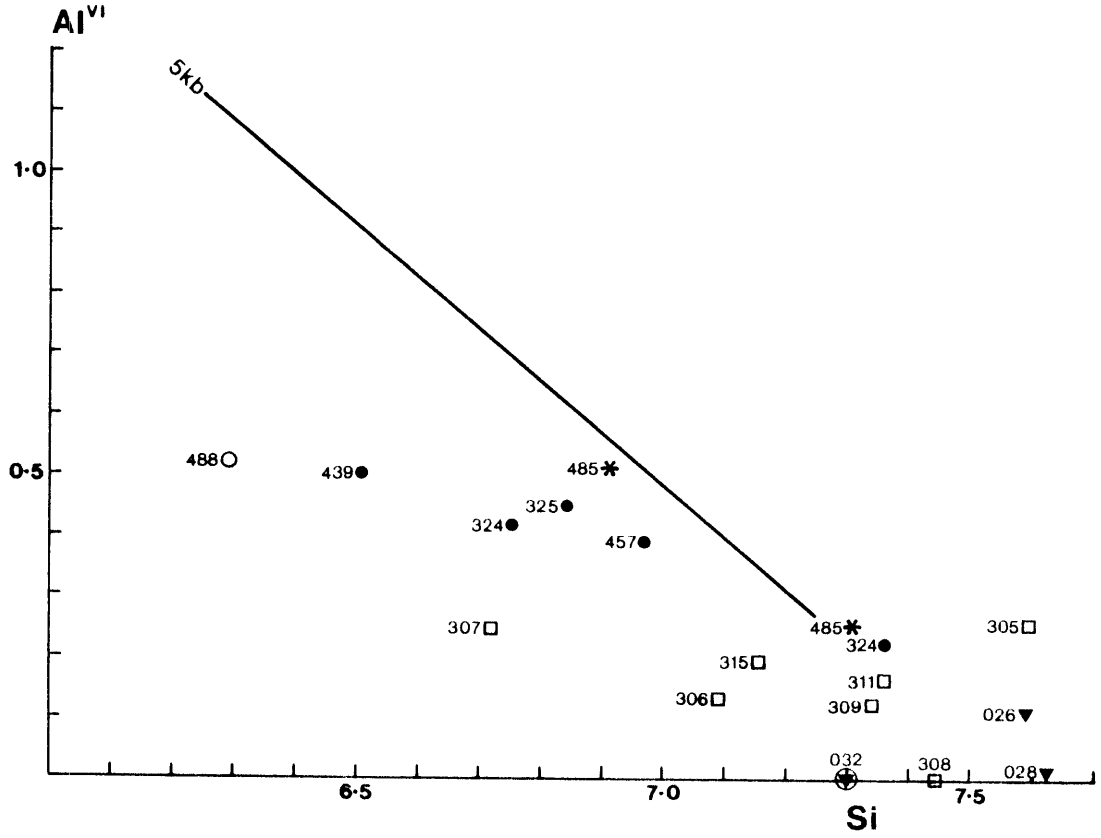

Fig. 5.8: Al^{VI}:Si relations in representative primary and secondary amphiboles from ophiolitic and exotic members of the PBOC. Hornblendes (Si 7.25) from low pressure metamorphic terranes usually plot below the 5kb line (*cf.* Raase, 1974). Sample numbers indicated on figure.
Amphiboles from the PBOC:

O amphibole-bearing harzburgite (primary tschermakitic hornblende)

✱ plagioclase-bearing peridotite

● olivine norites

▼ low-Ti gabbros

⊛ low-Ti dolerites

□ amphibolites

For amphibole analyses see Tables C-6 and 6.2.

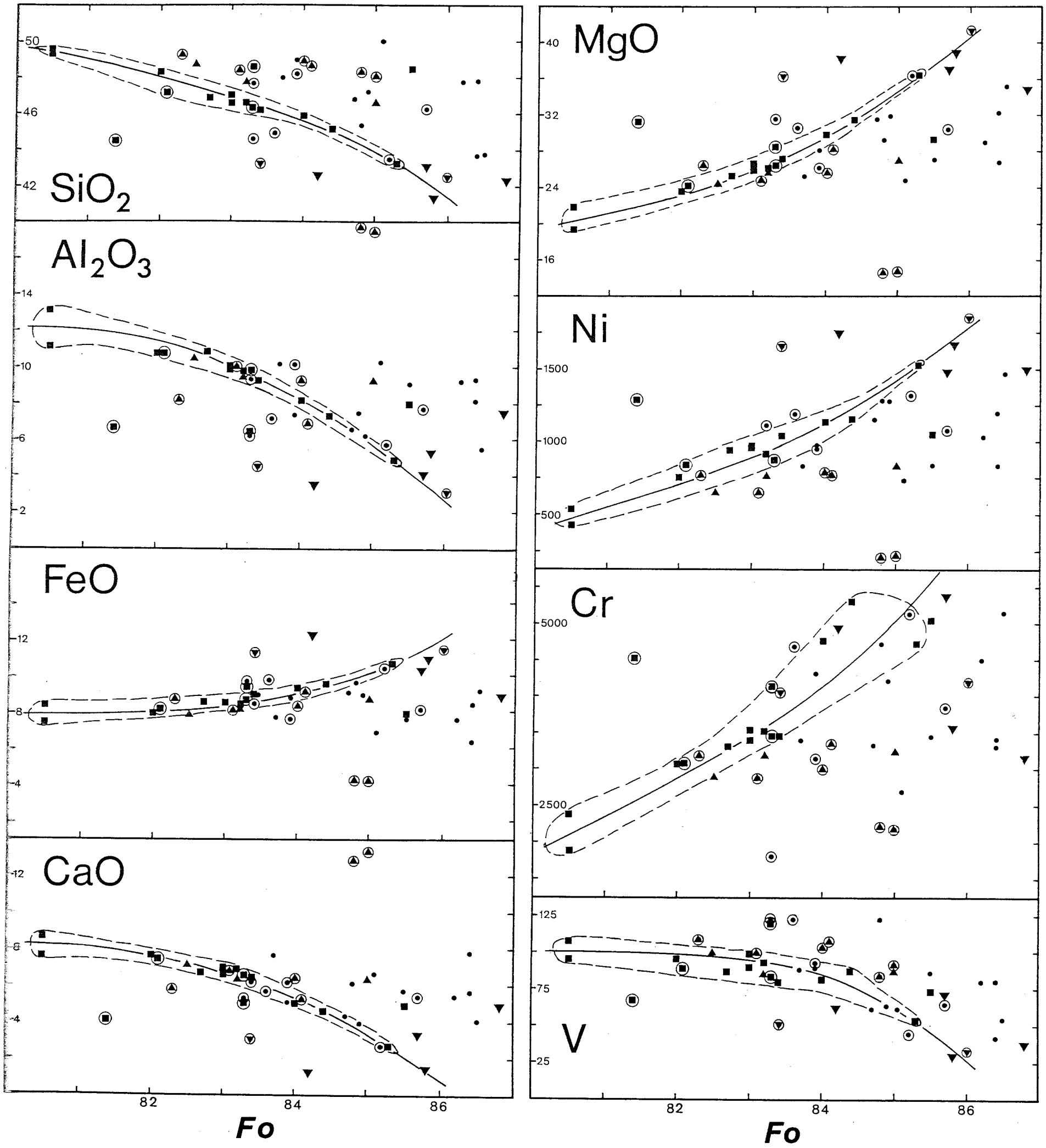

Fig. 5.9: Variations of selected major and trace elements in some PBOC olivine norites and plagioclase-bearing peridotites as functions of the measured or calculated Fo contents of their respective olivines.
Symbols:

▼ ⦿ plagioclase-bearing peridotites, localities 8,5,6,4,and 9 (in order of increasing Fo).

■ ◉ olivine norites, locality 3.

▲ ◬ " " , " 11, includes samples from two anomalously plagioclase-rich variants (samples 518, 520).

• ⊙ " " , other localities.

Circled symbols represent samples whose olivine compositions (Fo) have been calculated (see Appendix A and Section 5.4.4). Dashed fields include the majority of samples from locality 3 (see Section 5.4.4 and Figure 5.15 for discussions of some possible implications of these trends).

Figure 5.10: $\Sigma FeO:\Sigma FeO/MgO$ and $TiO_2:\Sigma FeO/MgO$ relations in ophiolitic members of the PBOC: a comparison with mafic and ultramafic lithologies from the ocean floor and other ophiolites.

PBOC: tectonized harzburgites (1), cumulate peridotites (2), olivine norites (3), low-Ti gabbros (●), low-Ti dolerites (▽), low-Ti basalts (4).

Ocean floor: 5 = harzburgites and serpentinized harzburgites (from analyses in Engel and Fisher, 1969; Miyashiro *et al.*, 1969; Aumento and Loubat, 1971; Bonatti *et al.*, 1971; Prinz *et al.*, 1976; Tiezzi and Scott, 1980).

OH = average of 235 oceanic harzburgites (Dmitriev *et at.*, 1976)

AH = average of 175 alpine-type harzburgites (Dmitriev *et al.*, 1976)

MORG = ocean floor gabbroic rocks (from analyses in Engel and Fisher, 1969,1975; Hekinian, 1970; Bonatti *et al.*, 1971; Blanchard *et al.*, 1976; Prinz *et al.*, 1976; Aumento *et al.*, 1977; Flower *et al.*, 1977; Perfit, 1977; Dostal and Muecke 1978).

a = MORG from the Ayu trough (Fornari *et al.*, 1979)

MORB = ocean floor basalt glasses. $\Sigma FeO:\Sigma FeO/MgO$ field modified from Bence *et al.* (1980). $TiO_2:\Sigma FeO/MgO$ field from Thompson *et al.* (1980).

Ophiolites: Fields from Beccaluva *et al.* (1979):-

VG = gabbroic rocks from Vourinos

LG = gabbroic rocks from the Internal Ligurides

TG = gabbroic rocks from Troodos

TB = sheeted dykes and Upper and Lower pillow Lava from Troodos

PG = gabbroic cumulates from Pindos (Capedri *et al.*, 1980)

PD = low-Ti doleritic intrusives from Pindos (Capedri *et al.*, 1980)

Skaergaard trend (Skd) from Miyashiro (1974).

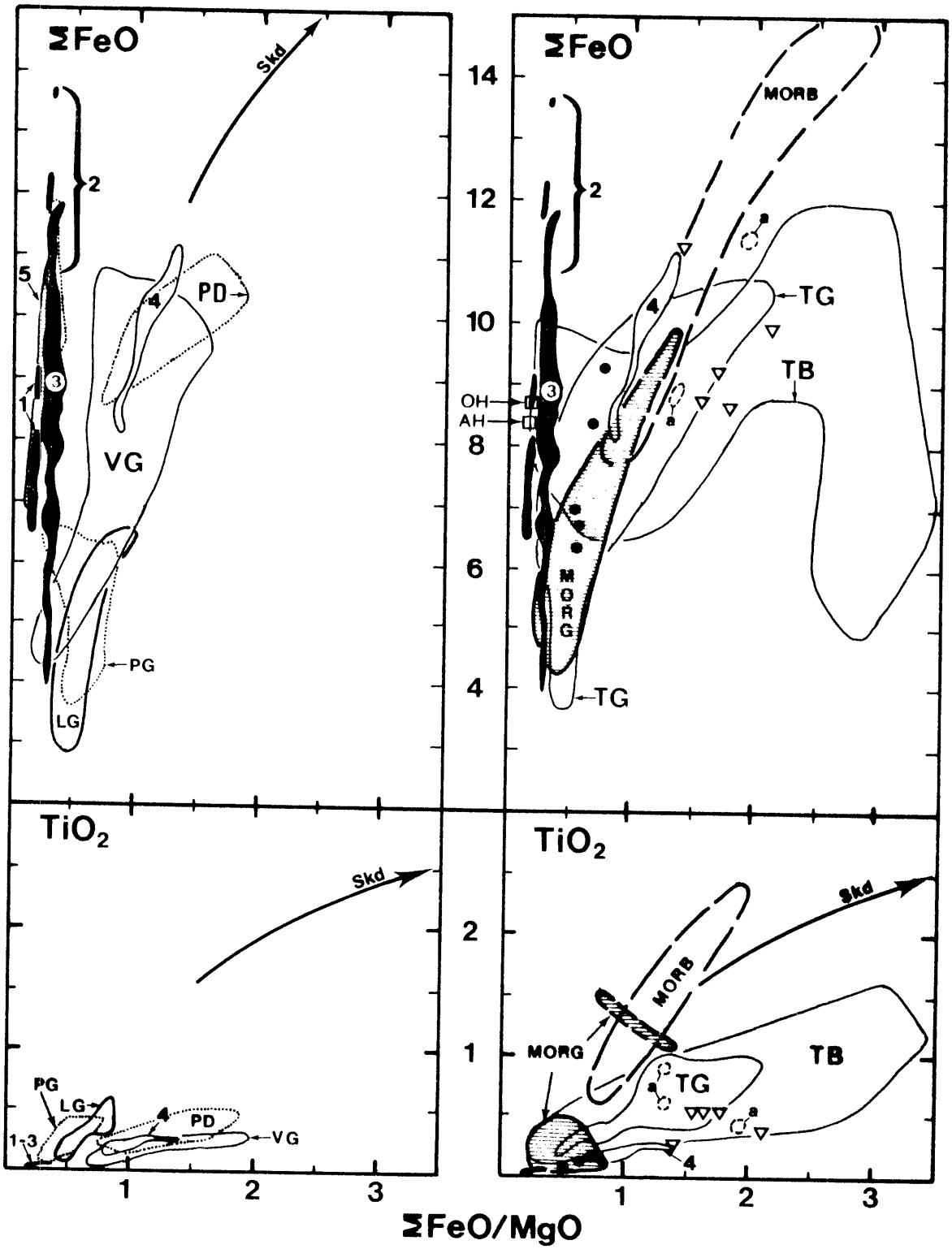
ΣFeO
Skd
2
5
4
PD
3
1
VG
PG
LG
ΣFeO
14
12
10
8
6
4
MORB
2
TG
4
TB
OH
AH
3
MORG
TG
TiO2
Skd
PG
LG
4
PD
VG
1-3
1
2
3
TiO2
2
1
Skd
MORB
MORG
TB
TG
4
1
2
3
ΣFeO/MgO

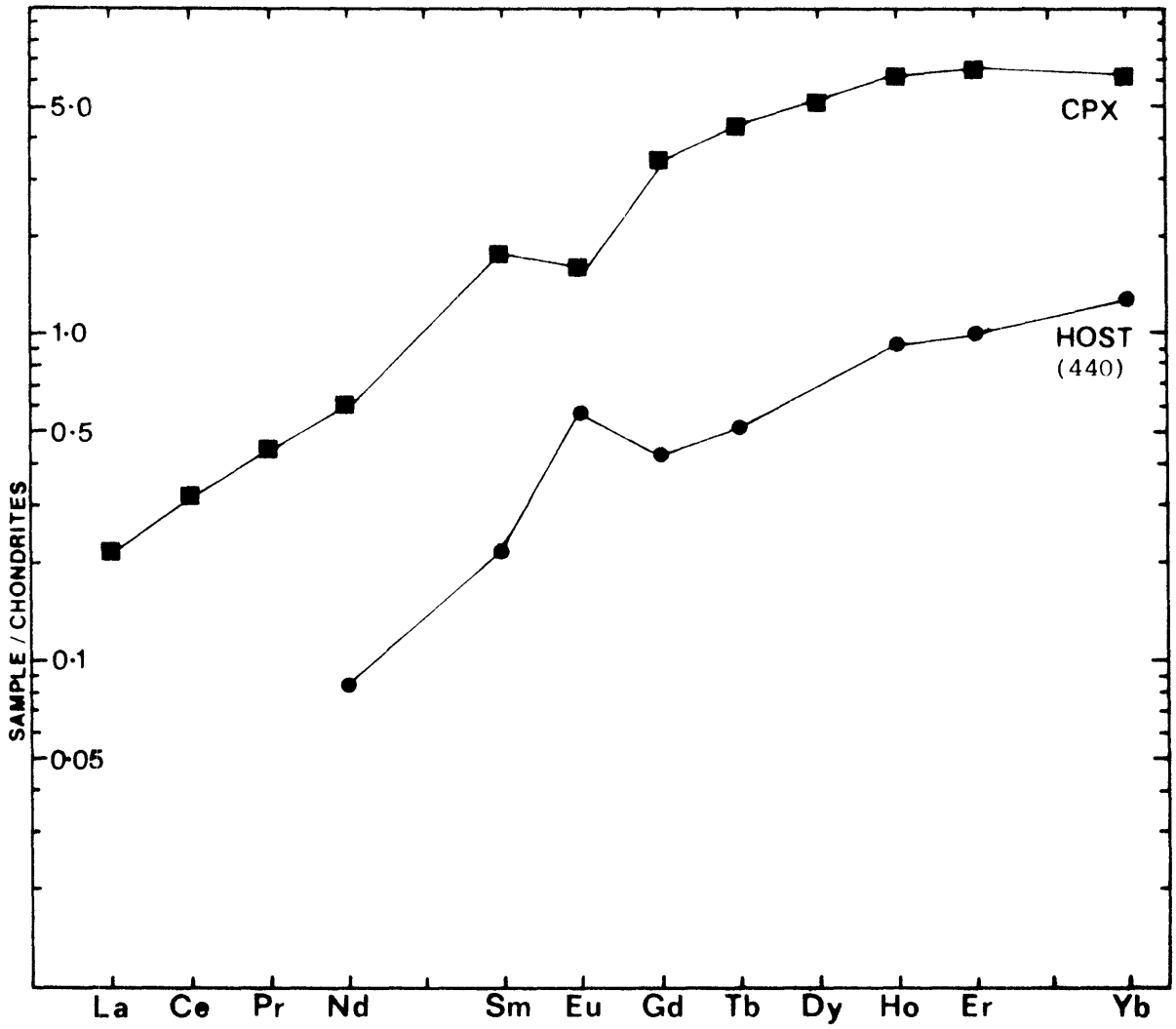

	La	Ce	Pr	Nd	Sm	Eu	Gd	Tb	Dy	Ho	Er	Yb
1.	0.08	0.31	0.06	0.43	0.41	0.14	1.05	0.25	1.95	0.52	1.60	1.55
2.	-	-	-	0.06	0.05	0.05	0.13	0.03	-	0.08	0.25	0.32

Fig. 5.11: REE abundances (ug/g) and chondrite-normalized REE distributions in PBOC olivine norite sample 440 and its Ca-rich pyroxene (CPX).

Analysis 1.=CPX and includes 1.5 ug/g Ba, 0.71 ug/g Pb.
Analysis 2.=HOST " " 0.9 " ", 0.16 " ".

Analyses by spark-source mass spectrometry.
Analyst S.R. Taylor, Research School of Earth Sciences, Australian National University.

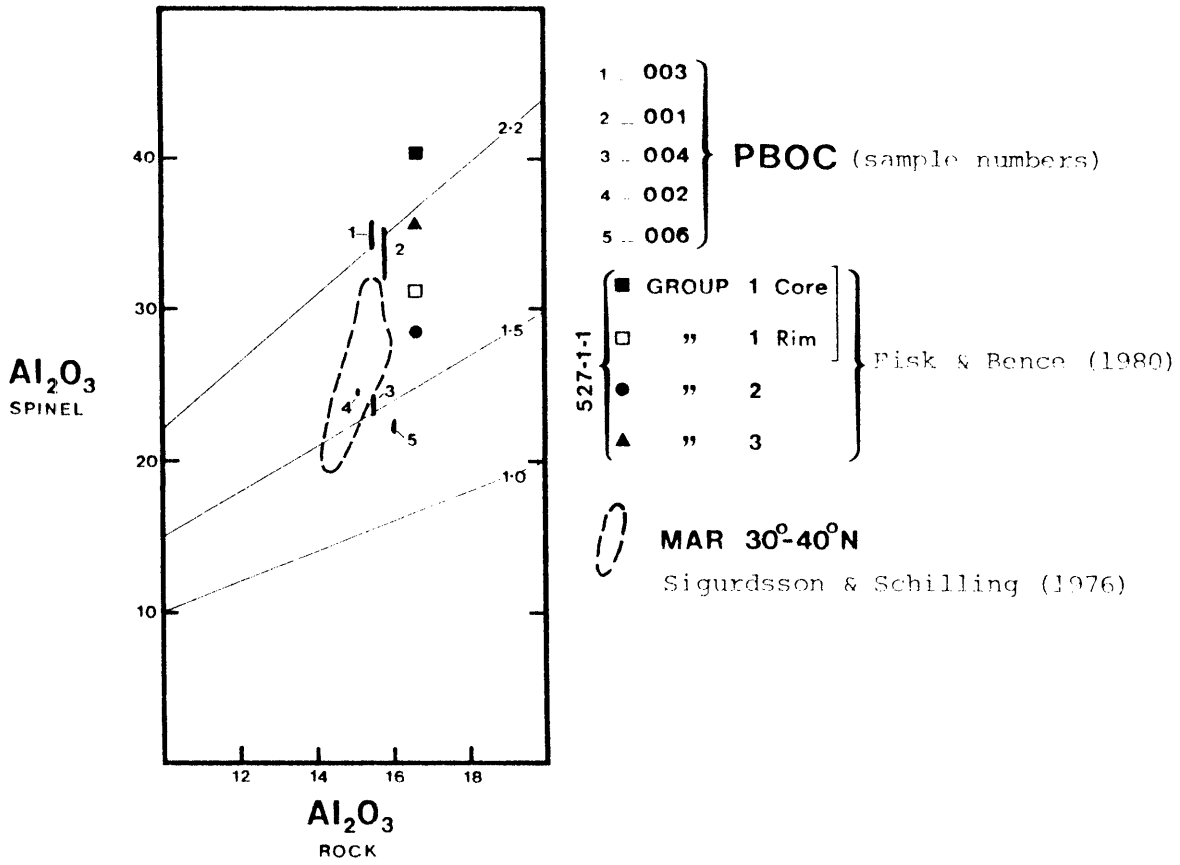

Fig. 5.12: Al_2O_3 contents of Cr-Al spinels in PBOC low-Ti basalts as a function of the Al_2O_3 contents of their respective hosts.

Figure 5.13A-D:

Selected major element characteristics of PBOC low-Ti basaltic rocks: comparisons with other 'depleted' basaltic types and a number of associated mafic and ultramafic rocks.

A: TiO_2x10:Al_2O_3:MgO relations

B: TiO_2x10:Al_2O_3:CaO relations

C: Si:Mg:Al relations; Fields C1-C4 for class 1 - class 4 basalts respectively (see Cameron and French, 1977).

D: Fe+Ti:Mg:Al relations, modified from Francis and Hynes (1979). Fields: UK=ultramafic komatiites; BK = basaltic komatiites; TH = tholeiites; CA = calc-alkaline rocks.

General Fields and Symbols:

1. Primitive and representative N-type MORB (many data sources; e.g. see J. Geophys. Res., Vol 81 No. 23, 1976; references in Sun *et al.*, 1979; Cann, 1981; Wilkinson, 1982).
2. PBOC low - Ti basalts
3. PBOC low - Ti gabbros
4. PBOC low - Ti dolerites
5. Miscellaneous ophiolitic - and other relatively low - Ti basaltic rocks e.g. Mings Bight, (Norman and Strong, 1975); Thetford (Sequin and Laurent, 1975; Church, 1977); Oman (Searle *et al.*, 1980, Pearce *et al.*, 1981). See also Sun and Nesbitt, 1978.
6. Troodos Upper pillow lavas and Arakapas low - Ti (boninitic) extrusives (Moores and Vine, 1971; Smewing *et al.*, 1975; Smewing and Potts, 1976; Simonian and Gass, 1978; Cameron *et al.*, 1979).
7. Betts Cove low - Ti basaltic extrusives (Coish, 1977; Coish and Church, 1979).
8. Khan Taishir low - Ti basaltic extrusives (Zonenshain and Kuzmin, 1978).
9. Boninites (Dallwitz *et al.*, 1966; Dietrich *et al.*, 1978; Kuroda *et al.*, 1978; Cameron *et al.*, 1979; Komatsu, 1980; Meijer, 1980; Shiraki *et al.*, 1980; Wood, 1980).
10. Komatiites and basaltic komatiites (Brooks and Hart, 1972; Hallberg and Williams, 1972; Gale, 1973; Bickle *et al.*, 1975; Arndt, 1977; Upadhyay, 1978; Francis and Hynes, 1979; Gansser *et al.*, 1979; Muir, 1979; Nesbitt *et al.*, 1979; Echeverria, 1980; Smith *et al.*, 1980).
11. Sao Paolo ridge, metabasalts and spilites (Fodor *et al.*, 1980).
12. Ferrobasalts and E - type MORB (Anderson *et al.*, 1975; Byerly *et al.*, 1976; Byerly, 1980; Ludden *et al.*, 1980; le Roex *et al.*, 1982; Schilling *et al.*, 1982).
13. Composite of fields 5 - 9.
14. Low - Ti doleritic rocks from the Aspropotamos sequence, Pindos (Capedri *et al.*, 1980).
15. Troodos upper pillow lavas + ultramafic extrusives (see 6, 23, 24).
16. Boninites and high - Mg andesites (see 9; Jenner, 1981; Tatsumi and Ishizaka, 1981).
17. Low - Ti (boninitic) extrusives, Arakapas (Simonian and Gass, 1978).
18. PBOC norite and peridotite cumulates.
19. Tamworth Belt basaltic rocks, Nundle and Morrisons Gap areas (Chapter 3).
20. Glen Ward basaltic rocks (Chapter 3).
21. Myra basaltic rocks (Chapter 3).
22. Average low - Ti basaltic extrusive, Baer-Bassit Ophiolite, Syria (Parrot, 1974, 1977).
23. Average ultramafic extrusive, Troodos (see 24).
24. Ultramafic upper pillow lavas, Troodos (Gass, 1958; Searle and Vokes, 1969; Desmet, 1976).
25. Average IAT (Basaltic Volcanism Study Project, 1981).
26. Average IAT, New Britain Arc (Basaltic Volcanism Study Project, 1981).
27. Calculated experimental equilibrium anhydrous melt compositions from Tinaquillo lherzolite starting composition (Jaques and Green, 1980).
    a. 11% partial melt at 10kb and 1250°C.
    b. 15% partial melt at 10kb and 1300°C.
    c. 17% partial melt at 2kb and 1200°C.

Fig. 5.13

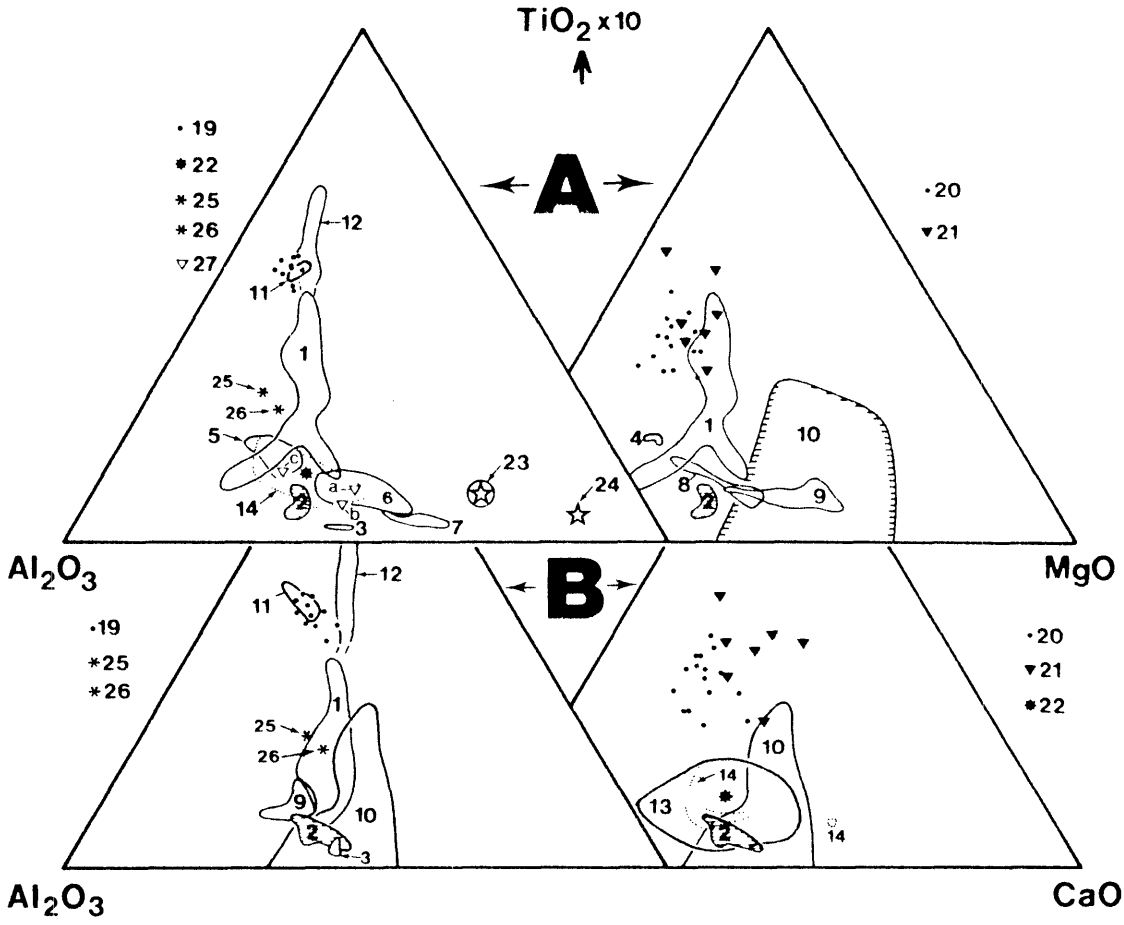
TiO2 x10
A
B
Al2O3
MgO
Al2O3
CaO
• 19
* 22
* 25
* 26
▽ 27
• 20
▼ 21
• 19
* 25
* 26
• 20
▼ 21
* 22

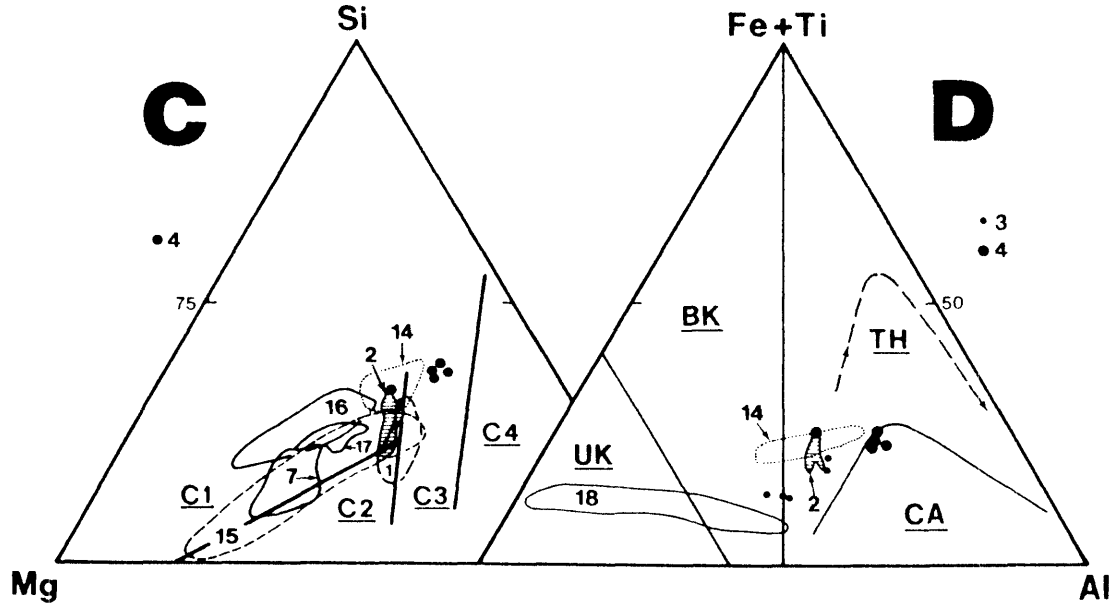
Si
Fe+Ti
C
D
Mg
Al
• 4
• 3
• 4
75
50
BK
TH
UK
CA
C1
C2
C3
C4

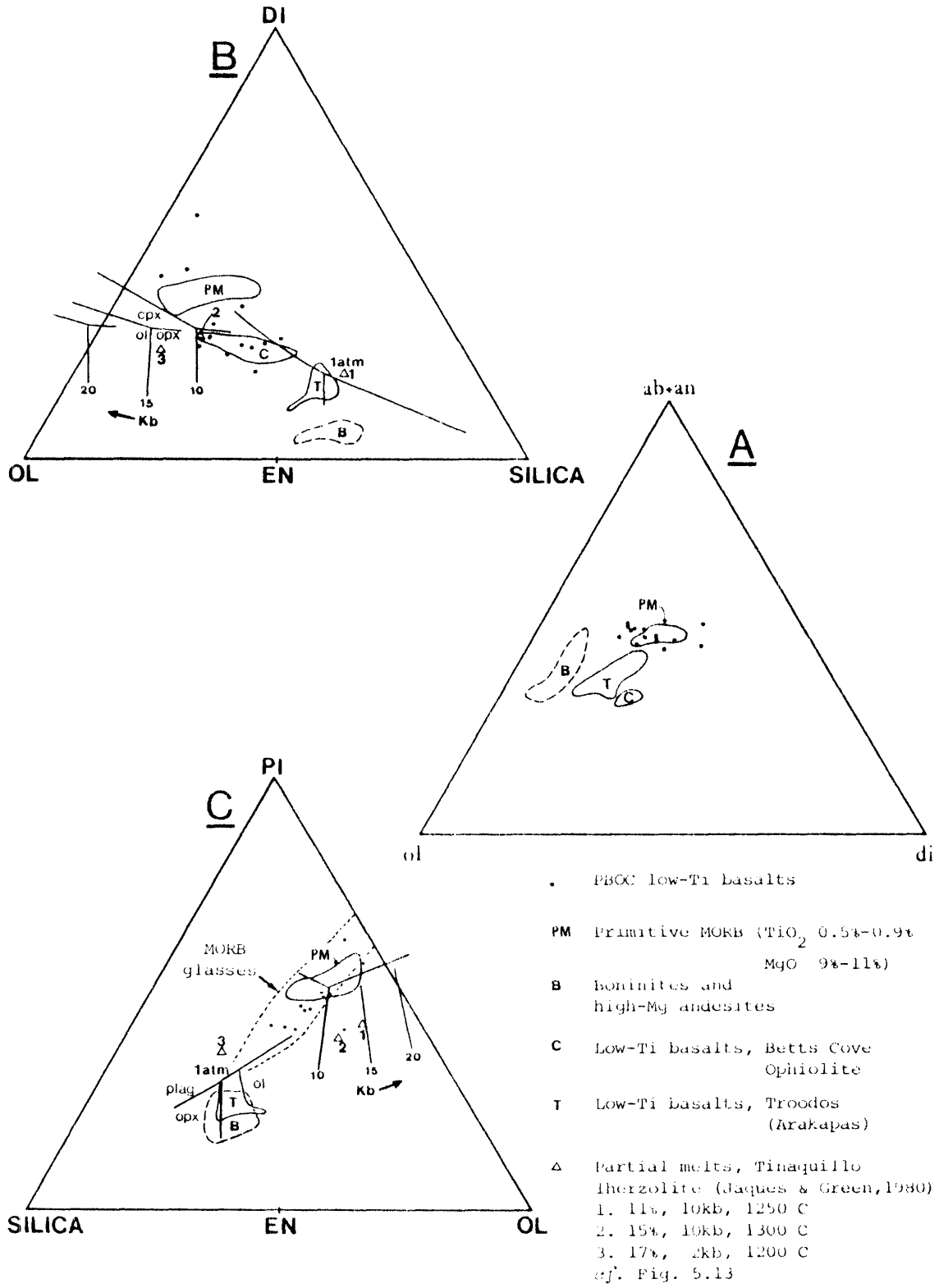

. PBOC low-Ti basalts

PM Primitive MORB (TiO_2 0.5%-0.9%, MgO 9%-11%)

B boninites and high-Mg andesites

C Low-Ti basalts, Betts Cove Ophiolite

T Low-Ti basalts, Troodos (Arakapas)

Δ Partial melts, Tinaquillo lherzolite (Jaques & Green, 1980)
1. 11%, 10kb, 1250 C
2. 15%, 10kb, 1300 C
3. 17%, 2kb, 1200 C
cf. Fig. 5.13

Fig. 5.14: Selected normative characteristics of PBOC low-Ti basaltic rocks and comparisons with some other basaltic compositions.
A: C.I.P.W. normative (*ab+an*):*ol*:*di* projection.
B: Projection from PL onto the plane DI:OL:SILICA.
C: Projection from DI onto the plane PL:SILICA:OL.

The normative parameters in B and C are those of Walker *et al.* (1979), and the experimental phase boundaries are from Stolper (1980). Other basaltic compositional fields are from references listed for Figure 5.13.

Fig. 5.15: Variations in selected major and trace element abundances in PBOC low-Ti basaltic (·) and doleritic (•) rocks. The solid trend lines are the loci of hypothetical liquid compositions calculated following the subtraction of small increments (0.5 wt%) of 'relevant' (see below) olivine norite compositions from low-Ti 'basalt' 010 (M = 64.2; analysis 10, Table 5.6a). The dashed trends are extrapolations of the calculated liquid lines of descent to hypothetical liquids whose M values are greater than that of 010 (i.e. M > 64.2)

Explanation: In this figure the M-related compositional trends displayed by the PBOC low-Ti basaltic rocks are compared with the trends which might be expected if the low-Ti basaltic rocks were related to the closely associated (locality 3) olivine norites by fractional crystallization processes.

From Figure 5.9 it is evident that, with relatively few exceptions, olivine norites at locality 3 (see Fig. B-1) display remarkably regular variations in bulk composition as functions of the Fo contents of their respective olivines. Assuming $D^{ol\text{-}liq.}_{Fe\text{-}Mg} \simeq 0.3$ (e.g. Roeder and Emslie, 1970) is appropriate to the assumed relatively low pressure (? $\ll$ 5kb, see Section 5.4) crystallization of these olivine norites, the more Mg-rich variants (e.g. sample 467, Mg* = 85.0, Fo = 85.3) most probably crystallized from melts whose M values were $\sim$ 63-64. Consequently, of the available PBOC low-Ti basaltic compositions (Table 5.6a), 010 (a sub-variolitic, essentially aphyric pillowed extrusive, M = 64.2) is the most magnesian variant from which the locality 3 olivine norites might have precipitated.

To assess the effects of fractionation of locality 3 olivine norite compositions from melts similar in composition to 010 a simple iterative procedure was employed, *viz*:

1. The approximate bulk composition* of an olivine norite whose olivine is potentially in equilibrium with 010 'melt' (i.e. Fo $\sim$ 85.6) was determined from the solid chemical trend lines in Figure 5.9 (composition A).
2. 0.5 wt% of 010 was removed as a cumulate fraction whose composition = A, and the composition of the residual liquid (010^1) recorded.
3. The Fo content of olivine in equilibrium with liquid 010^1 was calculated (assuming $D^{ol\text{-}liq.}_{Fe\text{-}Mg} = 0.3$) and an appropriate olivine norite composition (B) was determined from Figure 5.9.

Step (2.) was repeated for composition B and step (3.) for liquid 010^2 - and so on for M(liquid) = 64-54.

Thus the solid trend lines in Figure 5.15 represent the loci of liquid compositions 010-010^{12} (i.e. liquid compositions represented by steps 0-12). Clearly, most of these chemical trends (note especially the relative trends for Al_2O_3 and CaO, and Cr and Ni) are at variance with the overall trends displayed by the PBOC low-Ti basaltic rocks. Consequently, it is most unlikely that the olivine norites are complementary fractionates of these basaltic eruptives and minor intrusives (see text).

---

* The elements selected account for $\gg$ 98 wt% of the olivine norites under discussion, and $\sim$ 94-95 wt% of the liquids. Other significant components in the liquids (e.g. Na_2O and normalized Fe_2O_3) were treated as incompatible elements in the calculations.

FIG. 5.15

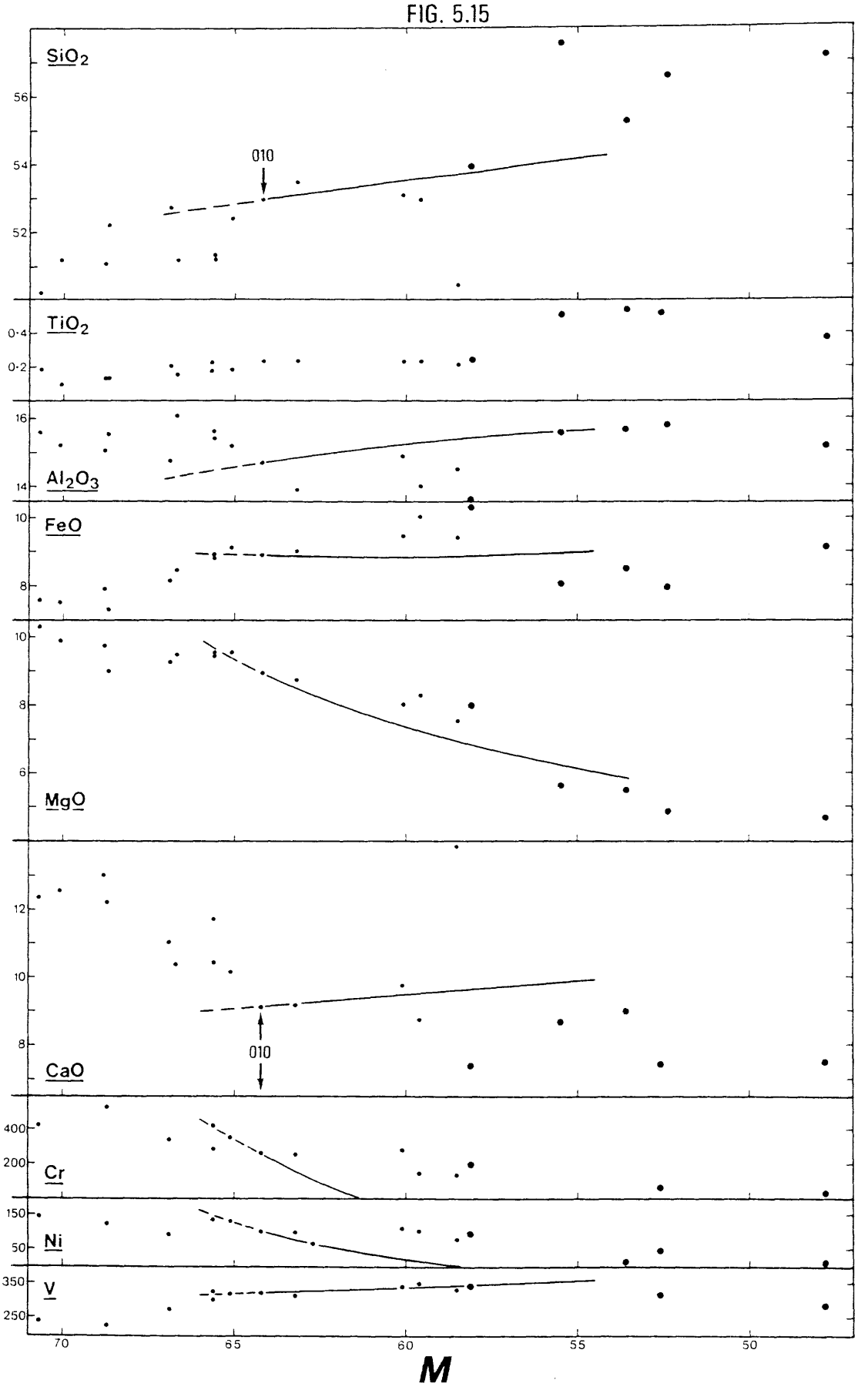
SiO2
56
54
52
010
TiO2
0·4
0·2
16
14
Al2O3
10
8
FeO
10
8
6
MgO
12
10
8
010
CaO
400
200
Cr
150
50
Ni
350
250
V
70
65
60
55
50
M

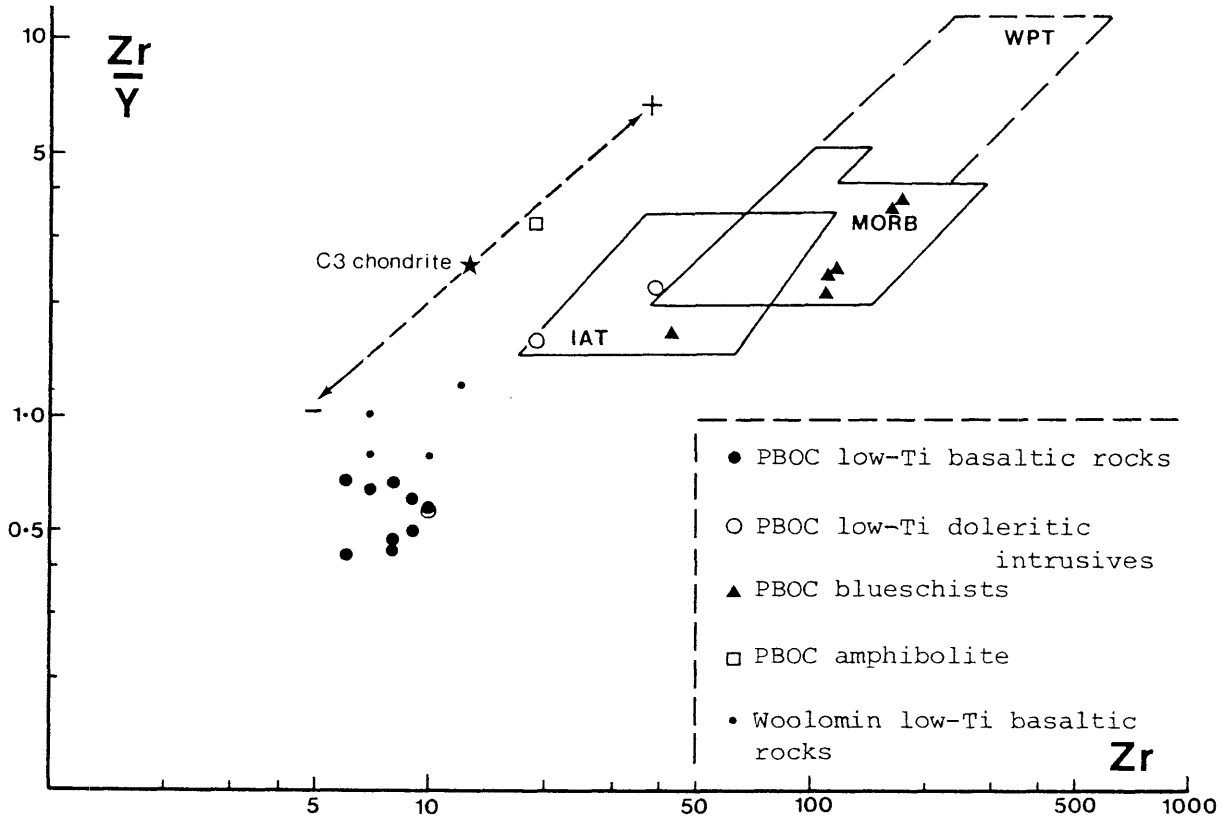

Fig. 5.16: Zr/Y:Zr relations in ophiolitic and exotic mafic members of the PBOC PBOC and in some low-Ti basaltic rocks from the Woolomin beds, Glenrock Station area (Offler, 1982). Fields after Pearce and Norry, (1979). Basalt source region enrichment (+) and depletion (-) trends relative to C3 chondrite (*cf.* Pearce 1980).

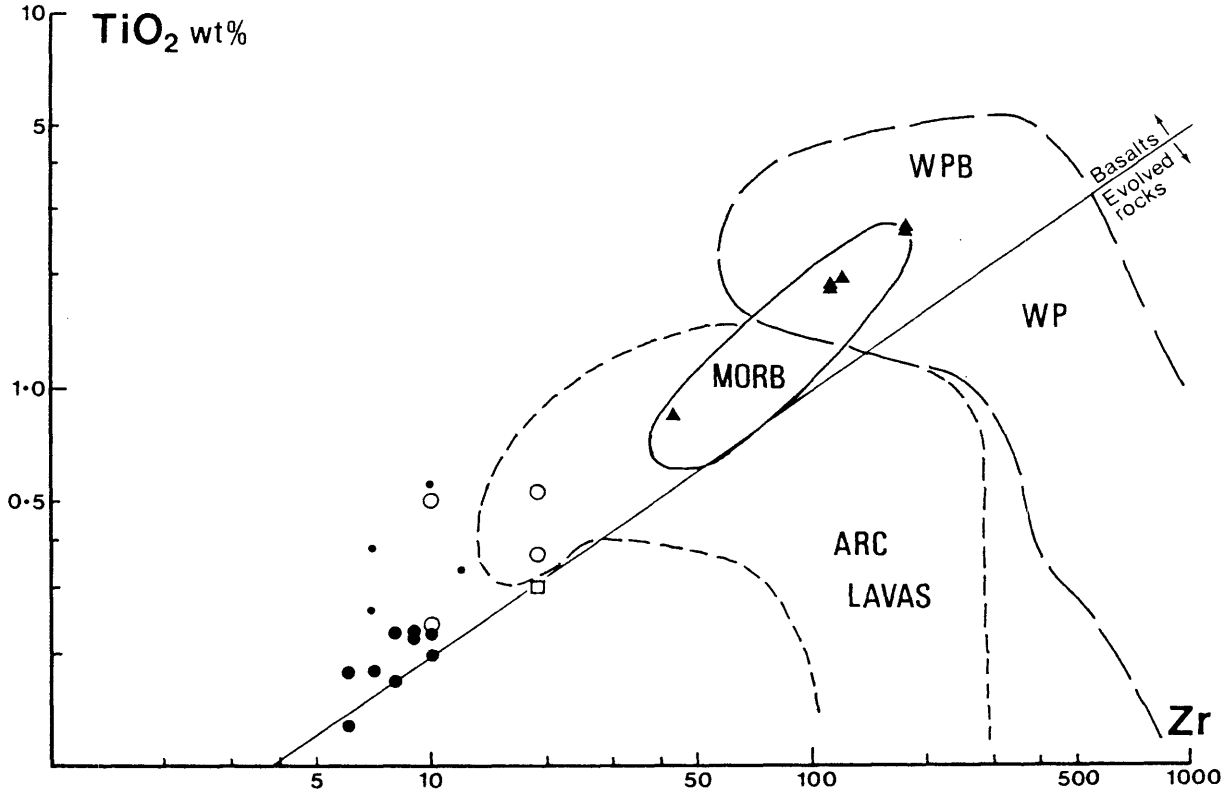

Fig. 5.17: TiO_2:Zr relations in ophiolitic and exotic mafic members of the PBOC and in some low-Ti basaltic from the Woolomin beds, Glenrock Station area (Offler, 1982). Fields after Pearce (1980); symbols as in Fig. 5.16.

CHAPTER 6

EXOTIC MEMBERS OF THE PBOC

In addition to relatively abundant fragments of ophiolitic lithologies (Chapter 5), the PBOC serpentinite-matrix melange also contains: (1) blocks which appear to have been derived tectonically from the adjacent rock associations; and (2) a range of amphibole-rich, relatively higher-grade metamorphic lithologies. Of these exotic blocks, only a selection of the fresher, relatively higher-grade types are examined in any detail (Section 6.2), and these only in a reconnaissance fashion.

6.1 LOW-GRADE, LOCALLY-DERIVED BLOCKS:

These include: (i) basaltic rocks, chert, jasper, siliceous argillite and rare volcanogenic epiclastics (e.g. GR634,823) which appear to have been derived from the Myra beds or the Glen Ward beds; (ii) tonalitic and hornblendite blocks from Pola Fogal Suite; and (iii) rare intermediate-silicic volcanics (e.g. GR650,815) which are probably derived from the Pitch Creek Volcanics. The locations of many of the more substantial tectonic blocks (> several tens of square metres in outcrop) are marked on Map 1. Some of these blocks have ostensibly eroded out of the surrounding schistose serpentinite, but most remain at least partially embedded in a matrix of highly schistose serpentinite (e.g. Plate 6.1A,B). Altered basaltic rocks are by far the most abundant of the block lithologies listed above and these are especially common in the PBOC schistose serpentinites lying along the Peel Fault System (Map 1).

Many of the locally-derived blocks have experienced at least some low-grade alteration over and above that developed in similar lithologies more-or-less adjacent to the PBOC. The basaltic and tonalitic blocks, in particular, have commonly experienced significant kaolinization (e.g. 318, 319; Plate 6.1A), chloritization (e.g. 320), uralitization (e.g. 317) and, on occasion, epidotization (e.g. 316; Plate 6.1B). In fact, many of the basaltic inclusions have a 'bleached' appearance in outcrop (e.g. Plate 6.1A) and this is largely due to pervasive kaolinization

of the plagioclase and the replacement of pyroxene by pale greenish amphibole and/or carbonate ± chlorite ± ?talc. For the most part, these basaltic inclusions are microdoleritic-doleritic types and their relict textures are similar to the majority of Glen Ward and Myra *Type 1* doleritic intrusives.

On present levels of exposure, uralitized basaltic rocks are rare in the Myra beds and exceedingly rare in the Glen Ward beds (Chapter 3, Section 3.3). Most of the PBOC low-Ti doleritic intrusives are highly uralitized (Section 5.6) but, unlike the uralitized doleritic inclusions in the serpentinite, these low-Ti types are usually quartz-bearing (Section 5.6) and their secondary amphibole is relatively deeper-green in colour. It is unclear whether the uralitized inclusions are fragments of Myra or (perhaps less likely) Glen Ward basaltic rocks originating from relatively deeper structural levels where uralitization might be widespread, or whether uralitization occurred after these blocks were incorporated in the serpentinite at depth (see Section 6.3).

Uralitized and lower-grade, and essentially unaltered "locally-derived" tectonic blocks are widespread throughout many schistose serpentinites in the NEO (e.g. Leitch, 1980a). Their modes of origin and alteration histories usually reflect: (i) relatively minor and apparently localized metamorphic and/or metasomatic events; and (ii) relatively high-level structural and tectonic events of small magnitude and rather localized significance. Secondary assemblages in blocks of this type have not been examined in any detail during the course of this study.

6.2 RELATIVELY HIGHER-GRADE METAMORPHIC BLOCKS

These are predominantly plagioclase-poor amphibolites and plagioclase-free hornblende schists, with minor relatively plagioclase-rich amphibolites, blueschists, mica (?stilpnomelane) schists and greenschists. Blocks of mica schist (e.g. 296, GR6996,8316; albite+quartz+stilpnomelane+muscovite+chlorite+zoisite) and greenschist (e.g. 294, GR6575,8198; ?actinolite+albite+chlorite+opaque oxide+sphene) are typically small (outcrops < 10 sq.m.), rare, and relatively insignificant. However, greenschist (314, albite+actinolite+chlorite+quartz) is locally abundant in association with amphibolites at GR707,829.

Fig. 6.1: Selected major and trace element relations in PBOC exotic rocks, low-Ti basalts and low-Ti doleritic intrusions. Low-Ti rocks from the Woolomin beds (Offler, 1982) plotted for comparison. For key to magma-type abbreviations see Appendix L.

a. Ti:Zr:Y relations. Fields from Pearce and Cann (1973) IAT = A+B, MORB = B, CAB = B+C, WPB = D.

b. Ti:Zr:Sr relations. Fields from Pearce and Cann (1973) IAT = A, CAB = B, MORB = C.

c. $\Sigma FeO:MgO:Al_2O_3$ relations. Fields from Pearce *et al.* (1977) 1 = MORB, 2 = OIT, 3 = CTB, 4 + Spreading Centre Island, 5 = Orogenic (IAT). Line a - b applies only to within-plate ocean island basalts and discriminates between tholeiitic (OITH) and alkaline (OIA) types.

d. $Zr/TiO_2:Nb/Y$ relations. Fields from Winchester and Floyd (1977) S-AB = subalkaline basalt, A,B = subalkaline andesite-basalt, A = andesite, R,D = rhyodacite - dacite, TA = trachyandesite, AB = alkaline basalt.

e. $Nb/Y:Zr/P_2O_5$ relations. Basalt fields from Floyd and Winchester (1975), Winchester and Floyd (1976). ALK = alkaline, TH = tholeiitic.

f. Ni:Y relations. MORB and IAT fields from Crawford and Keays (1978) NOTE sample 313 contains 292 µg/g Ni.

g. $TiO_2:Zr:P_2O_5$ relations. Fields for alkaline (ALK) and tholeiitic (TH) basalts from Winchester and Floyd (1976).

h. Cr:Y relations. Basalt fields from Pearce (1980). Line a - b is the locus of Cr:Y relations in partial melts derived by small (b,5%) to large (a,60%) degrees of partial melting of a hypothetical plagioclase lherzolite source (Pearce, 1980). O,Sp = olivine - spinel fractionation vectors (liquid lines of descent). NOTE sample 313 contains 1057 µg/gCr.

i. Ti/Cr:Ni relations. Fields for MORB and IAT from Beccaluva *et.al.* (1979).

j. Ti:V relations. Fields for MORB and IAT from Shervais (1982). B = boninite field compiled from references listed for Fig. 5.13.

NOTE: Low-Ti basaltic rocks are not plotted on diagrams d,e, and g. They fall well within the fields for subalkaline (tholeiitic) basalts on these three diagrams.

Fig. 6.1

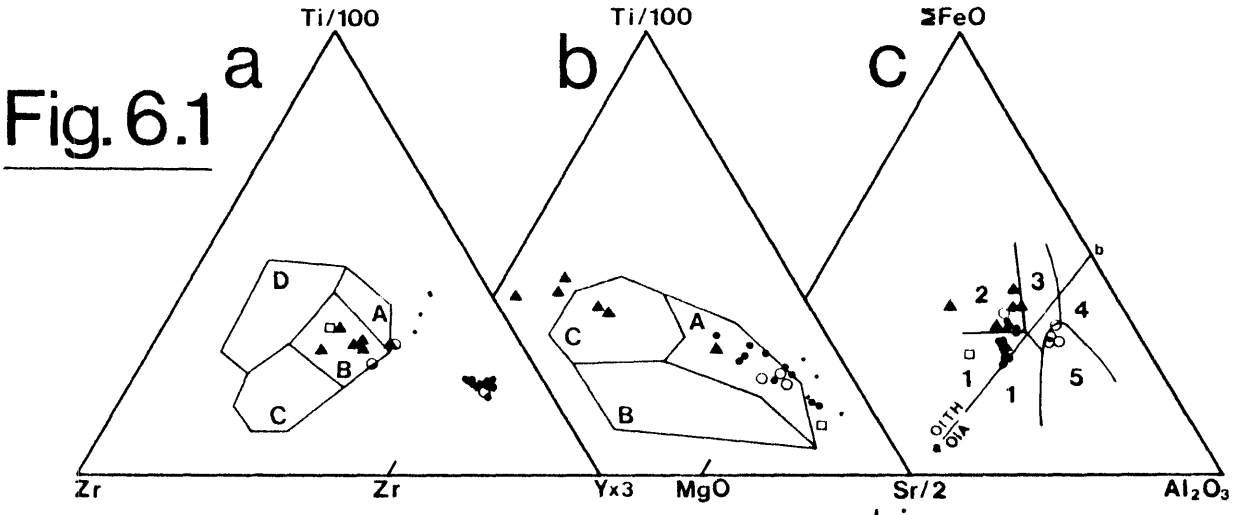

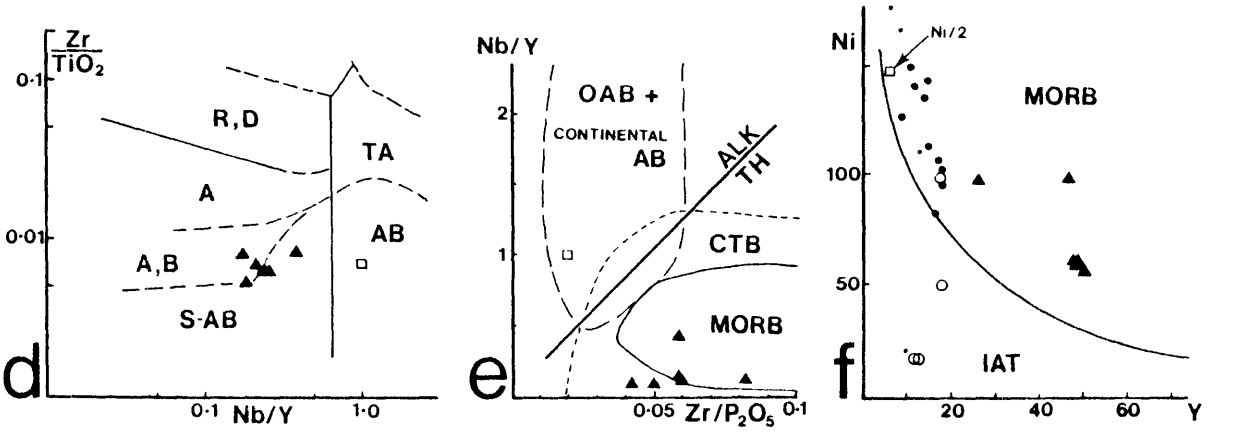

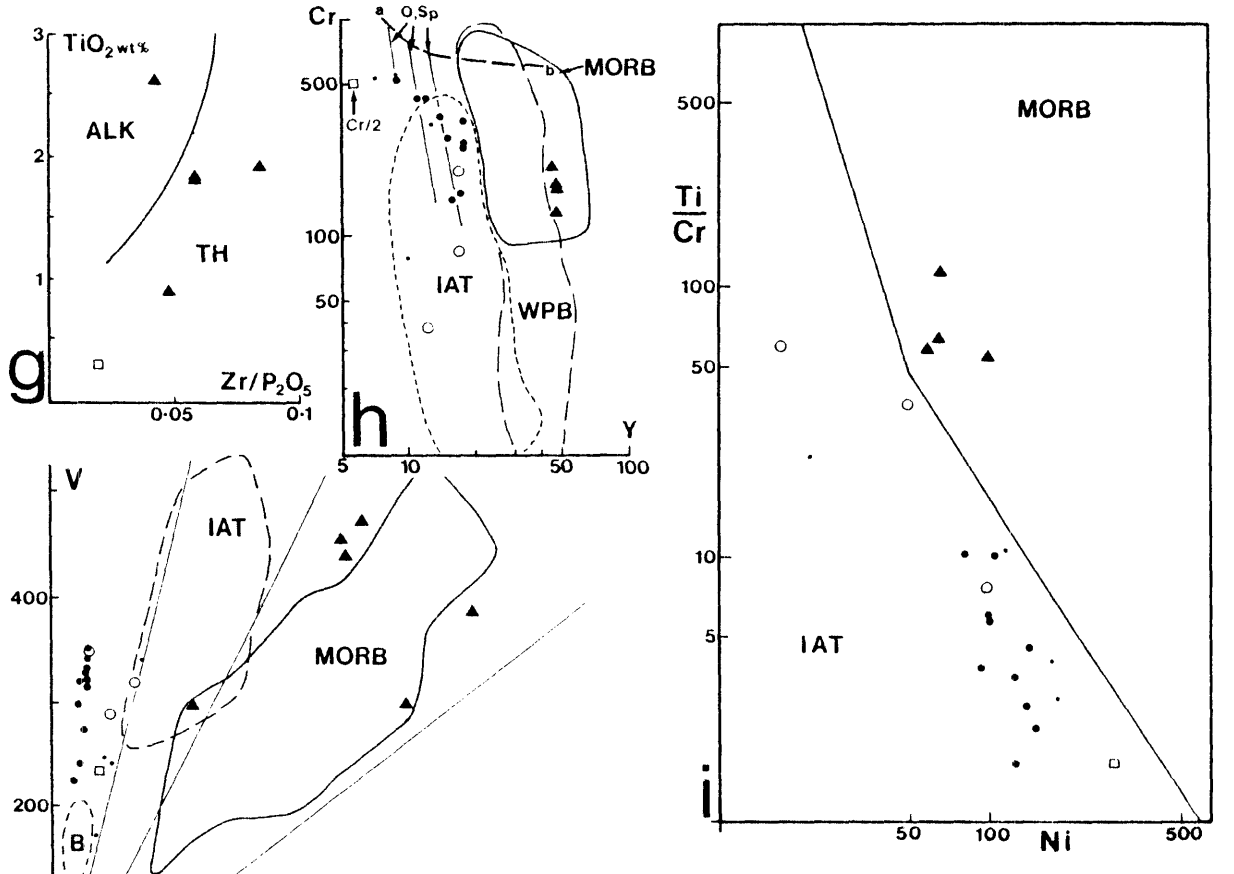

▲ PBOC blueschists

□ PBOC amphibolite (sample 313)

• PBOC low-Ti basalts

○ PBOC low-Ti doleritic intrusives

. Woolomin low-Ti basaltic rocks, Glenrock Station (Offler, 1982)

6.2.1 Amphibolites

(i) Plagioclase-poor types

Blocks of plagioclase-poor and plagioclase-free 'amphibolite' (e.g. 298, 311, 312) are relatively abundant in the PBOC schistose serpentinites. Most blocks of this type are clearly amphibolitized fragments of PBOC intrusives, and these have been discussed in Chapter 5. However, the mineral and/or whole-rock chemistries of a number of these blocks suggests that they were ultimately derived from precursors probably foreign to the PBOC (see below). For the most part, all three of the larger PBOC exotic amphibolite blocks (see Map 1) are poorly exposed. This poor exposure appears to be largely a function of widespread intense low-temperature shearing and subsequent pervasive weathering.

The largest of the predominantly plagioclase-poor amphibolite exotic blocks (block A) lies along the southeastern margin of a PBOC serpentinite in the vicinity of GR705,827 (see Map 1). Both block A and block B (see below) appear to be in fault contact with the adjacent Pola Fogal intrusives, and neither of these blocks are hornfelsed by the intrusives. In the vicinity of GR7011,8260, at least parts of this block consist of sedimentary rocks containing variable amounts of metamorphic (?metasomatic) amphibole. Partially amphibolitized interbedded argillites and sandstones are well-exposed at this locality. The thinner (<20cm) sandstone beds display well-developed graded-bedding but the thicker variants appear to be entirely amphibolitized, and recrystallization has obliterated sedimentary fabrics. Elsewhere in this block planar fabrics are relatively rare and, where developed they are often highly deformed (e.g. Plate 6.1C), and appear to be intrinsically metamorphic in origin. Some outcrops are massive although most display a well-developed, relatively low-temperature (cataclastic) shear foliation (Plate 6.1C) and, on occasion, an autoclastic melange fabric (Plate 6.1E). Disrupted albite±quartz±epidote (?metamorphic segregation) veins may be locally abundant, especially in the relatively finer-grained, strongly foliated variants (Plate 6.1D) and the greenschists.

The amphibolite block (block B) lying immediately to the southwest of block A (see Map 1) is also plagioclase-poor. Variants in this block are generally coarser-grained than those in block A, and pre-metamorphic fabrics are not recognizeable. Relatively small blocks

(tens of sq.m., or less) of similar amphibolites occur in schistose serpentinites immediately to the north of this large block (e.g. GR6881, 8205), and at numerous other localities throughout the PBOC (e.g. GR658, 822; GR690,888; GR707,832).

The plagioclase-poor amphibolites consist almost entirely of pleochroic pale-deep green, Mg-rich, relatively Al- and Na-poor calcic amphiboles (Table 6.1, analyses 9-13). In some samples (e.g. 309, 315) these 'hornblendes' are zoned to actinolitic rim compositions (Table 6.1, analyses 10-13). Modal plagioclase rarely exceeds 10% and is usually albitized and kaolinized. Accessory phases include prograde Ca-rich pyroxene (e.g. Table 6.2, analysis 6), relatively rare oxides, sphene and, in some samples, Mg-poor Cr-Fe spinel (Table 6.2, analyses 7 and 8). Vein- and minor secondary alteration phases include albite, actinolite, anthophyllite (e.g. 312), prehnite, epidote, chlorite, carbonate and sericite (after plagioclase, e.g. 312).

'Hornblendes' in these amphibolites are relatively Al-poor (Al_2O_3 2.5% - 6.3%, Table 6.1) and contain significantly less Al^{VI} (Fig. 5.8) compared to those in PBOC amphibolitized intrusives (Al_2O_3 5.3% - 12.0%, Table C-6). The relatively higher Al^{VI} and Na^{M4} contents of the secondary amphiboles in the PBOC olivine norites (e.g. Fig. 5.8) might suggest that these crystallized at somewhat higher pressures than those in the amphibolites. Recently, however, Hynes (1982) has demonstrated that these parameters can be unreliable indicators of pressures of amphibole crystallization in metabasites. 'Hornblendes' in both rock-types under discussion are highly depleted in TiO_2 (<0.12%). Although this is also consistent with relatively low pressures of amphibole crystallization (*cf.* Raase, 1974; Hynes, 1982), in these rocks bulk composition was probably the controlling factor in amphibole TiO_2-, and to a lesser extent, Al_2O_3 contents (see Table 6.3a, analyses 8 and 9; *cf.* Appendix B). Consequently, the data available do not closely constrain estimates of the pressures at which these plagioclase-poor amphibolites might have crystallized, especially as experimental and other data pertaining to relatively more Na-, Ti- and Al-rich 'basaltic' compositions are probably not strictly applicable to these particular lithologies.

The bulk chemistries of two of the PBOC plagioclase-poor

amphiboles (311, block A, and 312, block B; Table 6.3a analyses 8 and 9 respectively) suggest that these might be metamorphosed mela-gabbros. They are significantly enriched in *di* Table 6.3b), Ba, Zr and LREE, compared to PBOC ophiolitic intrusives with comparable MgO contents (*cf.* Tables 5.3 and B-7). Unlike the PBOC amphibolitized intrusives these amphibolites contain *prograde* (only) Ca-rich pyroxene which is significantly depleted in Cr and Al relative to relict pyroxenes in the former (Table 6.2, analysis 6; *cf.* Fig. 5.6). The Cr-Al spinels which occur in some of these amphibolites (e.g. 311, 315) are also chemically distinctive, being significantly enriched in Fe and Mn, and depleted in Al and Mg relative to those in the PBOC ophiolitic intrusives (Table 6.2, analyses 7 and 8; *cf.* Fig. 5.3, Table C-2).

The presence of chromite-bearing amphibolites (311), Cr-rich greenschists (314, 525 ug/g Cr, Table 6.3a, analysis 11) and partially amphibolitized argillites and sandstones (see below) in block A raises the possibility that this block, at least, might largely consist of metamorphosed mafic - ultramafic detritus which may or may not include a component derived from PBOC ophiolitic lithologies. Although the partially amphibolitized argillites and sandstones at GR7011,8260 are well-exposed, they were not sampled because they appeared to be too weathered and too friable for petrographic examination. Consequently their provenance is unknown but, in the light of the above discussion, they warrant further investigation.

(ii) Plagioclase-rich types

The largest block of relatively plagioclase-rich amphibolite in the Pigna Barney - Curricabark area (block C) crops out in the vicinity of GR675,821 (see Map 1). Small plagioclase-rich amphibolite blocks (tens of sq.m. or less) are embedded in schistose serpentinites at GR6895,8225 (306), and at GR577,945 (307). For the most part these amphibolites consist of highly irregular, mesoscopic, alternating amphibole-rich and plagioclase-rich layers, although relatively homogeneous and diffusely-banded types are common in block C (e.g. sample 313). Amphibolites from each of these three blocks are quite distinctive and some preliminary petrological data are summarized below.

Sample 306: a strongly foliated amphibolite containing approximately

60% pale olive-brown, Ti-bearing (0.8% TiO_2) magnesiohornblende (Table 6.1, analysis 7) and approximately 40% saussuritized plagioclase. Relict plagioclase is relatively calcic and uniform in composition (An_{82-78}, Table 6.1). Fe-Ti oxides are rare.

Sample 307: consists of highly irregular, elongate,medium-grained amphibole-rich patches and lenses in a banded matrix rich in altered (largely kaolinized) plagioclase (An_{30-25}, Table 6.1). Two types of amphibole are present: (i) a slightly pleochroic pale blue-green to pale brown to colourless amphibole (not analysed) forming relatively coarse-grained monomineralic patches; and (ii) a strongly pleochroic deep olive blue-green to pale olive-brown magnesio-alumino-kataphorite (Table 6.1, analysis 8; *cf.* Leake, 1978) which displays a granoblastic-elongate texture in association with plagioclase and relatively minor pale green Ti-poor salite (Table 6.2, analysis 5). Modal abundances of these three phases vary considerably, although salite rarely exceeds *ca* 10% of the mode. Sphene and rare opaque oxides are the only significant accessory phases.

Block C: These amphibolites largely consist of highly variable proportions of blue-green to pale olive-brown amphibole, and altered plagioclase. The latter is largely replaced by zoisite, clinozoisite, chlorite, prehnite±quartz±carbonate (more commonly in veins) assemblages. Mesoscopic patches of decussate pale-green amphibole are also relatively common in amphibolites forming this block (e.g. 293). The bulk chemistry of a composite sample (313) from a diffusely-laminated type (292) and a relatively massive type (291) displays some characteristics in common with relatively Mg-rich (MgO = 12.3%) 'basaltic' rocks. These include moderate Al_2O_3 (13.4%), high Ni (292 ug/g), high Cr (1057 ug/g), and low abundances of the relatively immobile incompatible elements (e.g. Zr, Nb, Y and, to a lesser extent P; Table 6.3a, analysis 10). However, the overall relatively immobile element relationships in this sample are not entirely consistent with any of the more common magma types. Thus Figure 6.1a,cj suggests subalkaline characteristics whereas Figure 6.1d,e suggests affinities with alkaline basaltic types. Rocks with comparable chemistry are unknown in the Tamworth Belt and the Woolomin Association. Also, this amphibolite is significantly enriched in *di*, TiO_2, P_2O_5, Zr, Ba LREE and Sr, and depleted in Al and *hy* relative to PBOC intrusives

PLATE 6.1

A. Tectonic block of highly kaolinized (?) microdolerite embedded in schistose PBOC serpentinite [sample 318, GR6205,8267].

B. Sub-rounded tectonic block of epidotized basalt in highly schistose PBOC serpentinite. Pale-coloured vein predominantly consists of prehnite + epidote [GR6832,8216].

C. Highly deformed PBOC amphibolite displaying a well-developed planar fabric. Note intense shearing in the upper right and left sides of the outcrop. [GR7065,8289].

D. Disrupted albite ± quartz ± epidote segregation veins in strongly foliated, fine-grained, PBOC plagioclase-poor greenschist [GR7066, 8288].

E. Autoclastic melange fabric in highly-sheared PBOC plagioclase-poor amphibolite. Pale patches (predominantly on phacoids) are moss or lichen [GR7066,8291].

F. Planar fabric (weakly developed glaucophane ± muscovite foliation) in PBOC blueschist delineated by thin segregation veins. These veins largely consist of albite + minor actinolite and muscovite [GR6567, 8189].

G. Small-scale disharmonic folds in segregation veins in PBOC blueschist [GR6567,8189].

H. Crenulations in foliated PBOC blueschist. The field of view consists of glaucophane (elongate) plus accessory sub-equant grains of sphene (dark grey-black).[sample 305, mag. = 35x , crossed nicols].

I. Glaucophane foliation wrapping around relatively early-formed garnets (large black grains) in PBOC blueschist. Pale alteration products after garnet are muscovite and pumpellyite. The garnets are largely altered to chlorite which is not resolvable in this photograph. [sample 299, mag. = 9x , crossed nicols].

PLATE 6·1

A

B

C

D

E

F

G

H

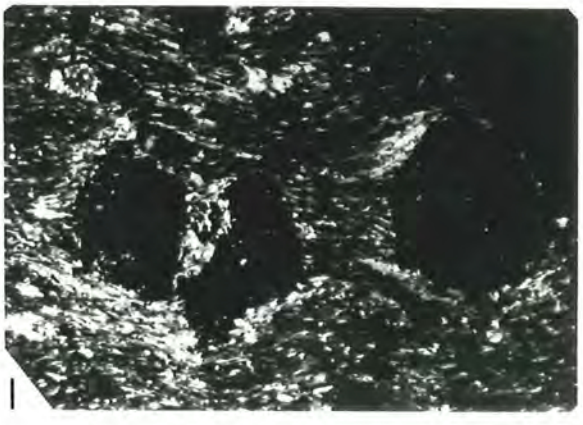

I

with similar MgO contents (*cf.* Table 5.4a,b, analyses 1-3) and, for that matter, practically all other PBOC ophiolitic lithologies (with the exception to the low-Ti doleritic intrusives which are, however, relatively depleted in Mg, Ni and Cr; Table 5.5a).

6.2.2 Blueschists

Blocks of glaucophane schist occur at three localities in the PBOC (1, GR6567,8190; 2, GR6573,8195; 3, GR6922,8271). The largest of these blocks (1) is marked on Map 1. It occupies the bed of the Pigna Barney River for approximately 200 metres and it ranges in width from approximately 20m to 40m. It displays a well-developed planar fabric [glaucophane (-muscovite) foliation; Plate 6.1F] which commonly strikes sub-perpendicular to the length of the block. However, this occurrence appears to be an aggregate of relatively small, somewhat jumbled sub-blocks and,consequently, present structural attitudes are of uncertain significance. Block 2 is small (1m. x 0.4m.), lensoidal, partially embedded in schistose serpentinite, and also in the bed of the Pigna Barney River. "Block" 3 consists of several relatively equant blocks ranging up to 20m in width which appear to have eroded out of the adjacent schistose serpentinite.

Overall assemblages in each of these occurrences include:

1. glaucophane (Table 6.1, analyses 1,2) + minor muscovite (Table 6.2, analysis 3), pumpellyite, garnet (Table 6.2, analyses 1,2) albite (An_{2-0}), calcite, relatively rare actinolite and/or chlorite, and accessory sphene, apatite, zircon and pyrite.

2. glaucophane + minor sphene, and accessory pumpellyite, pyrite and apatite.

3. glaucophane (Table 6.1, analyses 3-5) + sphene, minor albite, actinolite (Table 6.1, analysis 6), pumpellyite (Table 6.2, analysis 4), and accessory pyrite.

In block 1 albite and actinolite are largely confined to thin (?)segregation veins and lenses (Plate 6.1F) which usually lie within the plane of the glaucophane(-muscovite) foliation. Muscovite is also irregularly distributed. Although some of the segregation veins are disharmonically-folded on a relatively small scale (Plate 6.1G), there is little evidence for strong multiple deformation in block 1. On the

other hand, the glaucophane foliation in block 3 displays well-developed crenulations (Plate 6.1H), and has presumably experienced at least two distinct deformational episodes followed by cataclasis during (?) final emplacement.

Relict (largely chloritized) garnets in block 1 are almandine-grossular solid solutions (Table 6.2, analyses 1,2) containing ~20% pyrope+ spessartine+andradite end-members. In general terms these are compositionally similar to garnets characteristic of relatively high-grade blueschist assemblages (e.g. Newton and Fyfe, 1976; Turner, 1981) and Group C (alpine-type) eclogites (Coleman *et al.* 1965; Raheim and Green, 1975; Ryburn *et al.* 1976). However, the PBOC blueschists appear to be devoid of the more diagnostic high-pressure phases such as jadeite, lawsonite, aragonite and omphacite, and the presence of relatively abundant sphene + calcite rather than rutile also suggests relatively low-grade, blueschist facies conditions of metamorphism (Ernst, 1972; Blake and Morgan, 1976; Hunt and Kerrich, 1977; Itaya and Banno 1980). Textural relations suggest that the garnet predates the glaucophane foliation (Plate 6.1I) and, as such, it might be relict from an earlier, largely obliterated, higher-grade blueschist facies assemblage. Constraints on the stability of glaucophane (Maresch, 1977), and recent generalized blueschist facies P-T phase diagrams of Wood (1979), Brothers and Yokoyama (1982) and Brown and O'Neil (1982), all suggest that the typical PBOC assemblage: glaucophane+sphene+albite+muscovite, in the absence of jadeite, crossite and lawsonite (or its high temperature breakdown product *viz* zoisite± pyrophyllite; Liou, 1971; Nitsch, 1972; Kushev, 1980), probably crystallized under P-T conditions in the vicinity of 400°C and 6-8kb. Rb-Sr isotopic data on muscovite separated from block 1 (Table H-2) suggest that this particular assemblage is Early Devonian in age (378 m.y.).

Although metamorphic segregation processes have probably produced significant chemical heterogeneities in these PBOC blueschists, for the most part their bulk chemistries (Table 6.3a, analyses 1-6) strongly suggest that they were originally basaltic rocks. Apart from their relatively low Al_2O_3:MgO + ΣFeO + Al_2O_3 ratios (Fig. 6.1c), which most probably reflect some segregation of Al into albite veins, and the relatively high TiO_2 (2.6%) and P_2O_5 (0.4%) abundances in sample 303 (Fig. 6.1g), most relatively immobile element characteristics of these blueschists resemble those typically displayed by subalkaline basalts,

and in particular, E-type MORB (e.g. Figs 5.16, 5.17, 6.1a,b,d-j). In many of these characteristics blueschists from blocks 1 and 3 resemble Myra *Type 1* basaltic rocks (Table 3.5a, analyses 1,2; compare Figs. 5.17, 5.18, 6.1 with Figs 3.2-3.33). On this basis, and bearing in mind that the Myra beds are probably part of a relatively widespread subduction complex (see Chapter 1), it is conceivable that the TiO_2-rich blueschists might have been ultimately derived from subducted Myra *Type 1* basaltic rocks or their equivalents. On the other hand, Ti, Zr, Nb and Y abundances in the block 2 blueschist (300) compare more closely to those in some Glen Ward basaltic extrusives (compare analysis 1, Table 6.3a with analyses 2 and 3, Table 3.7) than abundances of these elements in Myra basaltic rocks. However, the latter have significantly greater $\Sigma FeO/MgO$ ratios than the former (300) and, by analogy with other Glen Ward basaltic rocks (Table 3.6a), they may well be significantly enriched in P, V, LREE, and depleted in Ni and Cr relative to this blueschist. Thus, the available chemical data impose few tangible constraints on the ultimate origin of block 2, especially in view of the relatively large range of basaltic rock types known to occur in the Woolomin Association as a whole (see Chapter 3, Section 3.5).

6.3 DISCUSSION

Rare, isolated exotic blocks of blueschist and higher-grade metamorphics occur in a number of serpentinites in the NEO. These appear to be most abundant in the Pigna Barney - Curricabark, Glenrock Station and Port Macquarie areas (this thesis; Barron *et al.*, 1976; Leitch 1980c; Offler, 1982b), although blocks of amphibolite have been reported from serpentinites in the Mount George and Toms Creek areas (Leitch, 1980a) and in the Woodsreef area (Glen and Heugh, 1973). Other exotic metamorphic blocks associated with serpentinites in the Peel Fault System and in Zone B include: (i) mafic eclogites near Attunga (Shaw and Flood, 1974) and at Port Macquarie (H.D. Hensel, pers. comm.); (ii) possibly the nephrite occurrences approximately 25km southeast of Tamworth (Hockley, 1974; Lanphere and Hockley, 1976; and (iii) blueschists at several other unspecified localities (H.D. Hensel, pers. comm.).

Because these exotic blocks typically occur in serpentinite-matrix melanges delineating major fault systems in the NEO, their tectonic

implications must remain uncertain. However, by analogy with other ophiolites, at least some of these metamorphic blocks might be tentatively interpreted as remnants of sub-ophiolitic metamorphic soles ('dynamothermal aureoles' *cf.* Church and Stevens, 1971; Williams and Smyth, 1973; Graham and England, 1976; Malpas, 1979) fragmented during the emplacement of NEO serpentinites and related rocks.

Many ophiolites are directly underlain by thin (<<1km) highly deformed granulite- or amphibolite facies assemblages which pass rapidly into low-grade and/or unmetamorphosed rocks further away from the base of the overlying ophiolite. In various ophiolites such metamorphics have been recently interpreted to have formed: (i) within the oceanic crust prior to obduction [e.g. Ballantrae Complex, Spray and Williams, 1980; Treloar *et al.* 1980; Mamonia Complex, Cyprus, Spray and Roddick 1981; Hellenic (Greek) ophiolites, Spray and Roddick, 1980]; or (ii) from MORB and/or sedimentary rocks accreted to the base of the ophiolite during obduction (e.g. Bay of Islands and related Newfoundland ophiolites, Dallmeyer and Williams, 1975; Dallmeyer, 1977; Malpas, 1979; Jamieson, 1980; Feininger, 1981), or accreted during subduction (e.g. some Tethyan ophiolites, Hall, 1980; Searle and Malpas, 1980,1982; Thuizat *et al.*, 1981; and some ophiolites in the southwestern Pacific, Parrot and Dugas, 1980). On occasion, one or other of all three of the above interpretations have been specifically applied to individual dynamothermal aureoles beneath a number of the Tethyan ophiolites (compare Woodcock and Robertson, 1977; Hall, 1980; Thuizat *et al.*, 1981). The common lack of consensus highlights the uncertainties commonly encountered in evaluating the mode(s) of origin of such rocks.

Metamorphic rocks which have presumably originated *via* one or other of the above mechanisms may become incorporated in serpentinite-matrix melange zones within the ophiolite itself. In some parts of the Semail ophiolite of Oman, for instance, 'exotic' metamorphic blocks within serpentinite-matrix melanges may be correlated with metamorphic 'soles' underlying the ophiolite elsewhere (Searle and Malpas, 1980, 1982). However, in highly disrupted ophiolites it is not uncommon for a range of such metamorphic associates to be preserved only as rare and widely-scattered exotic blocks in ophiolitic melange [e.g. Taurus suture zone, Turkey, Hall, 1976,1980; Kings - Kaweah ophiolite, California

(largely oceanic fracture zone metamorphism), Saleeby, 1977,1978,1979; Oman, Searle and Malpas, 1980,1982; New Caledonia, see Parrot and Dugas (1980) for a summary] and, like those in the PBOC,their origin(s) may be difficult to assess.

The limited petrological data available on the PBOC exotic metamorphic blocks indicate that they are a polygenetic group largely derived from mafic igneous parents and, rarely, sedimentary rocks. The PBOC blueschists, at least, and blocks of blueschist and eclogite in other NEO serpentinites (see above), are probably subduction-related (*cf.* Ernst, 1971,1973,1977) and it is conceivable that these might have been ultimately derived from a range of somewhat MORB-like Woolomin Association basaltic rocks (see Sections 1.1, 3.6.1,6.2.2). Isotopic ages obtained on PBOC and Port Macquarie blueschist blocks (Rb-Sr 378 m.y., this study, Appendix H; K-Ar 383=5 m.y., Port Macquarie, Pogson and Hilyard, 1981) are similar and suggest that subduction and perhaps accretion occurred in Zone B at least in the Early Devonian. On the other hand, nephrites from serpentinites in the Peel Fault System 25km to the south of Tamworth have Early Permian $^{40}Ar/^{39}Ar$ ages (273 ± 6m.y., 280 ± 6 m.y., Lanphere and Hockley, 1976) but the precise geological relevance of these 'nephrite ages' is uncertain. The data are obviously too few to establish whether the blueschists and nephrites were formed during separate metamorphic events or whether they simply reflect piecemeal sampling of metamorphic rocks generated during a prolonged subduction event (*cf.* Cawood, 1982a).

If, as appears likely (see Chapter 7), the PBOC was generated in an outer-arc or remnant arc setting, conventional concepts of ophiolite emplacement (see above) might not be entirely applicable. Exotic amphibolite blocks in the PBOC are chemically distinct from MORB (see Section 6.2), as is at least one amphbolite block at Port Macquarie (Table 6.3a, analysis 7), and consequently these are probably not metamorphosed fragments of oceanic crust. Perhaps some of these amphibolite blocks and associated greenschists were initially generated as metamorphic soles to ophiolitic slabs accreted at depth in the Woolomin Association. Similarly, the blueschists and uralitized basaltic blocks (see Section 6.1) in the PBOC and elsewhere in the NEO might represent altered fragments of such ophiolitic slabs themselves. Because relatively higher-temperature

metamorphic overprinting of the PBOC blueschist assemblages is minimal (minor actinolite), it is likely that these exotic blocks, at least, were transported to relatively high structural levels within a geologically short period (?<50 m.y., *cf.* Draper and Bone, 1981) after their generation. However, the data available impose few constraints on mechanisms whereby these blocks might have been finally mixed with PBOC ophiolitic lithologies. A complex interplay of strike-slip and thrusting movements during, and perhaps following, accretion in Zone B is conceivable (see Chapter 1, *cf.* Karig, 1980).

TABLE 6.1

Representative Analyses of Amphiboles from Metamorphic Rocks in the PBOC

ANALYSIS No.	1	2	3	4	5	6	7	8	9	10	11	12	13
	Blueschists						Amphibolites →			CORE	RIM	CORE	RIM
SAMPLE	301	302	305	305	305	305	306	307	311	309	309	315	315
SiO_2	56.46	54.16	53.92	54.45	56.17	51.96	48.99	45.64	52.42	51.55	55.25	50.70	55.06
TiO_2	0.19	-	-	0.32	0.13	-	0.78	0.66	0.05	-	-	0.12	-
Al_2O_3	10.57	11.17	7.18	11.19	8.87	3.85	6.12	8.75	4.84	4.66	0.83	6.26	2.50
Cr_2O_3	-	-	-	-	-	-	0.21	-	0.09	0.19	-	0.38	0.06
ΣFeO	12.83	13.27	16.39	15.48	16.93	15.39	14.46	15.14	7.05	10.43	8.95	7.84	6.53
MnO	0.11	0.12	0.16	0.18	0.16	0.23	0.08	0.25	0.05	0.23	0.52	0.05	-
MgO	9.03	9.19	9.53	7.60	7.69	13.18	14.45	12.89	19.39	17.18	17.87	18.53	20.46
CaO	1.23	2.63	4.89	2.02	1.32	11.53	11.34	11.49	12.24	12.28	12.47	12.22	12.47
Na_2O	6.83	7.39	4.63	6.46	6.78	1.19	0.96	3.51	0.88	0.52	0.29	1.08	0.44
K_2O	-	0.08	0.05	-	-	0.09	-	0.10	-	0.08	-	0.14	0.05
TOTAL	97.25	98.01	96.75	97.70	98.05	97.42	97.39	98.43	97.01	97.12	96.19	97.32	97.57
Fe_2O_3	1.37	0.22	2.20	1.72	2.20	1.10	5.27	1.37	3.58	4.55	0.51	3.96	2.43
FeO	11.60	13.07	14.41	13.93	14.95	14.40	9.72	13.91	3.83	6.33	8.49	4.27	4.35
New Total	97.39	98.03	96.97	97.37	98.27	97.53	97.92	98.57	97.37	97.57	98.24	97.71	97.82
Numbers of cations on the basis of 23 (O,OH)													
Si	7.888	7.638	7.792	7.699	7.936	7.592	7.087	6.724	7.363	7.341	7.925	7.153	7.661
Al^{IV}	0.112	0.362	0.208	0.301	0.064	0.408	0.913	1.276	0.637	0.659	0.075	0.847	0.339
Al^{VI}	1.629	1.495	1.015	1.564	1.413	0.255	0.131	0.243	0.164	0.123	0.065	0.194	0.071
Ti	0.020	-	-	0.034	0.014	-	0.085	0.073	0.005	-	-	0.013	-
Cr	-	-	-	-	-	-	0.024	-	0.010	0.021	-	0.042	0.007
Fe^{3+}	0.144	0.023	0.239	0.183	0.234	0.121	0.574	0.152	0.378	0.488	0.055	0.420	0.254
Fe^{2+}	1.355	1.542	1.741	1.648	1.767	1.760	1.176	1.713	0.450	0.754	1.019	0.504	0.506
Mn	0.013	0.014	0.020	0.022	0.019	0.029	0.010	0.031	0.006	0.028	0.063	0.005	-
Mg	1.880	1.932	2.052	1.602	1.619	2.870	3.116	2.830	4.060	3.647	3.619	3.897	4.244
Ca	0.184	0.397	0.757	0.306	0.200	1.805	1.758	1.814	1.842	1.874	1.916	1.847	1.859
Na	1.850	2.021	1.297	1.771	1.857	0.337	0.269	1.003	0.240	0.144	0.081	0.295	0.119
K	-	0.014	0.008	-	-	0.017	-	0.019	-	0.015	-	0.025	0.008
Σ	15.075	15.438	15.129	15.130	15.123	15.194	15.143	15.878	15.155	15.094	15.018	15.242	15.068
M	0.581	0.556	0.541	0.493	0.478	0.620	0.726	0.623	0.900	0.829	0.789	0.885	0.893
Fe^*	0.081	0.015	0.191	0.105	0.142	-	-	-	-	-	-	-	-
An	<2	<2	n.f.	n.f.	n.f.	n.f.	78-82	25-30	n.f.	n.f.	n.f.	<2	<2

Fe^{3+} calculated following the method of Papike *et al.* (1974)

$M = Mg/(Mg+Fe^{2+})$

$Fe^* = Fe^{3+}/(Fe^{3+}+Al^{VI})$

An = Anorthite content of co-existing plagioclase

n.f. = not found

Analyses 1-5 = glaucophane
6,11 = actinolite
7,12 = magnesio-hornblende
8 = magnesio-alumino-kataphorite
9,13 = actinolitic-tremolitic hornblende
10 = actinolitic hornblende

Amphibole nomenclature after Leake (1978).

Plagioclase-rich amphibolites: 306 & 307
Plagioclase-poor amphibolites: 309,311,315

TABLE 6.2

Microprobe Analyses of some Minor Mineral Phases in Metamorphic Rocks from the PBOC

ANALYSIS No.	1	2	3	4		5	6	7	8
	Blueschists					Amphibolites			
SAMPLE	299	299	301	305		307	311	311	315
SiO_2	37.13	37.36	48.79	37.09		51.71	52.60	-	-
TiO_2	0.33	-	0.41	-		-	0.12	0.20	0.40
Al_2O_3	21.39	21.18	27.84	25.88		1.34	1.29	7.21	5.18
Cr_2O_3	0.18	-	-	-		-	-	51.43	34.19
$*Fe_2O_3$	1.13	1.79	n.d.	n.d.		7.51	1.04	9.10	28.46
FeO	23.85	24.19	3.40	3.67		1.89	8.35	30.12	30.09
MnO	3.06	2.54	-	0.61		0.26	0.13	0.76	1.52
MgO	2.06	2.19	3.16	3.00		12.75	14.20	1.32	0.53
CaO	10.98	10.93	-	22.57		22.90	22.24	-	0.15
Na_2O	-	-	0.50	0.40		1.64	0.16		-
K_2O	-	-	10.61	-		-	-	-	-
TOTAL	100.11	100.18	94.71	93.24		100.00	100.13	100.14	100.52
Oxygens	24	24	22	28		6	6	32	32
Si	5.884	5.917	6.617	6.807		1.925	1.959	-	-
Al^{IV}	0.116	0.083	1.383	0.117		0.059	0.041		
Al^{VI}	3.800	3.870	3.067	5.481		-	0.016	2.415	1.771
Ti	0.039	-	0.042	-		-	0.003	0.043	0.087
Cr	0.023	-	-	-		-	-	11.556	7.843
Fe^{3+}	0.135	0.213	-	-		0.210	0.029	1.946	6.214
Fe^{2+}	3.162	3.205	0.386	0.564		0.059	0.260	7.168	7.311
Mn	0.411	0.341	-	0.095		0.008	0.004	0.183	0.374
Mg	0.487	0.517	0.639	0.821		0.707	0.788	0.559	0.229
Ca	1.864	1.855	-	4.438		0.913	0.888	-	0.047
Na	-	-	0.131	0.142		0.118	0.012	$(0.130)^{\dagger}$	$(0.124)^{\dagger}$
K	-	-	1.836	-		-	-	-	-
Σ	15.921	16.001	14.101	18.465		3.999	4.000	24.000	24.000
mg	11.6	12.1	62.3	55.5		71.8	72.9	5.7	1.6
Cr	n.d.	n.d.	n.d.	n.d.		n.d.	n.d.	82.7	81.6
AL	53.2	54.2			*Ca*	48.1	45.1		
SP	6.9	5.8			*Mg*	37.3	40.0		
PY	8.2	8.7			*Fe'*	14.6	14.9		
AN	4.4	5.4							
GR	26.4	25.9							
UV	0.6	-							

$*Fe_2O_3$ calculated †cation ratios for Zn

n.d. = not determined

Analyses 1,2 = garnet; 3 = muscovite; 4 = pumpellyite; 5,6 = salite; 7,8 = chromite.

Analysis 7 includes 0.62% ZnO

Analysis 8 includes 0.58% ZnO

TABLE 6.3a

Major and Trace Element Analyses of Metamorphic Rocks Associated with the Pigna Barney Ophiolitic Complex

	Blueschists						Amphibolites				G'schist
ANALYSIS No.	1	2	3	4	5	6	7	8	9	10	11
SAMPLE	300	301	302	303	304	305	310*	311	312	313	314
SiO_2	49.70	49.17	49.48	50.64	46.54	50.25	56.61	52.24	52.65	46.63	61.43
TiO_2	0.84	2.20	1.83	2.62	1.94	1.82	0.01	0.08	0.04	0.30	0.17
Al_2O_3	14.24	12.58	13.10	12.86	14.93	12.90	1.35	4.76	5.77	13.37	11.30
V_2O_3	0.04	0.04	0.06	0.06	0.07	0.07	0.01	0.01	0.02	0.03	0.02
Cr_2O_3	n.d.	0.03	0.03	0.02	0.02	n.d.	0.23	0.35	n.d.	0.15	0.08
Fe_2O_3	1.59	2.16	2.66	2.79	2.66	2.90	1.18	2.13	1.96	1.73	1.75
FeO	8.07	8.61	10.05	9.72	10.77	10.35	4.54	5.14	7.82	7.20	5.29
NiO	0.01	0.01	0.01	0.01	0.01	0.01	0.16	0.09	0.04	0.04	0.01
MnO	0.19	0.18	0.20	0.18	0.22	0.20	0.19	0.16	0.30	0.17	0.03
MgO	8.73	8.44	7.30	6.81	6.94	6.24	21.14	19.33	15.06	12.28	9.15
CaO	10.70	7.41	8.55	6.56	9.06	7.30	11.02	11.50	11.82	12.23	3.06
Na_2O	2.17	3.54	3.49	4.82	2.83	4.34	1.24	0.93	0.93	1.64	3.12
K_2O	0.47	1.13	0.35	0.48	0.37	0.13	0.20	0.30	0.61	0.33	0.45
P_2O_5	0.09	0.28	0.19	0.41	0.14	0.19	0.02	0.06	0.05	0.10	0.07
ΣVol[1]	3.01	3.73	3.06	3.28	3.87	3.54	2.69	2.81	2.40	4.15	3.54
TOTAL	99.85	99.51	100.36	101.26	100.37	100.24	100.59	99.89	99.47	100.35	99.47
ΣFeO/MgO	1.09	1.25	1.70	1.80	1.90	2.08	0.26	0.37	0.64	0.71	0.75
TRACE ELEMENTS (µg/g)											
Rb	11	15	<2	5	4	<2	<2	<2	16	<2	5
Ba	109	388	55	120	73	27	-	91	131	116	64
Sr	182	25	115	90	146	62	40	323	29	257	82
Li	10.5	10.5	9.9	12.7	9.9	12.7	2.2	4.4	1.1	7.2	8.3
Zr	43	163	111	174	117	110	<2	27	13	19	43
Nb	5	16	10	9	11	12	<3	7	3	6	8
Y	26	46	48	47	48	50	3	5	4	6	5
Ti[1]	5240	11702	10059	15285	10796	11028	163	267	210	1798	1175
Cu	32	18	70	58	87	55	20	3	8	33	8
Zn	65	105	120	118	128	118	60	45	80	78	65
Ni	92	99	60	66	66	57	1231	719	302	292	94
Co	55	n.d.	n.d.	n.d.	n.d.	63	71	87	79	71	55
V	298	301	439	387	468	453	53	58	123	233	143
Cr	n.d.	207	171	129	166	n.d.	1560	2364	n.d.	1057	525
La	4	16	-	-	12	14	-	5	4	6	6
Ce	-	28	-	-	21	18	-	9	6	15	12
Nd	-	18	-	-	14	14	-	4	-	4	7

* FROM Pt. MACQUARIE N.S.W.

[1] See Appendix G

n.d. = not determined.

PBOC

Blueschists

Block 1 : analyses 2-5
Block 2 : analysis 1
Block 3 : analysis 6

Amphibolites & Greenschist

Block A : analyses 8 & 11
Block B : analysis 9
Block C : analysis 10

TABLE 6.3b

C.I.P.W. Normative Mineralogy of Metamorphic Rocks Associated with the Pigna Barney Ophiolitic Complex

	Blueschists						Amphibolites				Greenschist
ANALYSIS No.	1	2	3	4	5	6	7	8	9	10	11
SAMPLE	300	301	302	303	304	305	310*	311	312	313	314
qz	-	-	-	-	-	-	2.95	-	0.71	-	16.85
or	2.78	6.68	2.07	2.84	2.19	0.77	1.18	1.77	3.60	1.95	2.66
ab	18.36	29.95	29.53	40.87	23.95	36.81	5.83	7.8	7.87	13.88	26.40
an	27.75	15.13	19.10	12.05	27.00	15.34	-	7.95	9.80	28.17	14.72
c	-	-	-	-	-	-	-	-	-	-	0.29
di	20.21	16.18	18.26	14.72	14.14	16.35	43.20	38.82	39.12	25.74	-
hy	20.80	7.51	12.13	4.76	8.76	10.91	41.88	33.46	34.21	4.14	33.25
ol	3.57	13.72	10.18	14.74	14.24	10.45	-	5.27	-	19.87	-
mt	1.54	1.66	1.97	1.95	2.09	2.09	-	1.13	1.55	1.41	1.10
chr	-	0.04	0.03	0.02	0.03	-	0.44	0.52	-	0.22	0.12
il	1.60	4.18	3.48	4.98	3.68	3.46	0.02	0.15	0.08	0.57	0.32
ap	0.21	0.65	0.44	0.95	0.32	0.44	0.05	0.14	0.12	0.23	0.16
Vol	3.01	3.73	3.06	3.28	3.87	3.54	2.69	2.81	2.40	4.15	3.54
Σ	99.83	99.43	100.25	101.16	100.27	100.16	100.64	99.82	99.46	100.33	99.41
100 an/(ab+an)	60.2	33.6	39.3	22.8	53.0	29.4	-	50.3	55.5	67.0	35.8

$Fe^{3+}/\Sigma Fe = 0.1$

* From Port Macquarie, New South Wales

total includes:- 1.79 acmite

0.61 Na metasilicate